Panovska, S., Constable, C., Brown, M. (2018): Global and Regional Assessments of Paleosecular Variation Activity Over the Past 100 ka. - *Geochemistry Geophysics Geosystems (G3)*, *19*, 5, pp. 1559—1580.

DOI: http://doi.org/10.1029/2017GC007271

AGU100 ADVANCING EARTH AND SPACE SCIENCE

Geochemistry, Geophysics, Geosystems

RESEARCH ARTICLE
10.1029/2017GC007271

Global and Regional Assessments of Paleosecular Variation Activity Over the Past 100 ka

S. Panovska[1,2], C. G. Constable[1], and M. C. Brown[2,3]

[1]Institute of Geophysics and Planetary Physics, Scripps Institution of Oceanography, UCSD, La Jolla, CA, USA, [2]GFZ German Research Centre for Geosciences, Potsdam, Germany, [3]Institute of Earth Sciences, University of Iceland, Reykjavík, Iceland

Key Points:
- New data compilation of paleomagnetic, archeomagnetic, and lava flow data over the past 100 ka is presented
- Regional stacks of PSV index show a more pronounced Laschamp excursion in the Northern versus Southern, and in the Atlantic versus Pacific Hemispheres
- Global and regional stacks show no anomalous activity at the time of the Mono Lake excursion or other excursions during the past 100 ka

Supporting Information:
- Supporting Information S1

Correspondence to:
S. Panovska,
panovska@gfz-potsdam.de

Citation:
Panovska, S., Constable, C. G., & Brown, M. C. (2018). Global and regional assessments of paleosecular variation activity Over the Past 100 ka. *Geochemistry, Geophysics, Geosystems*, *19*, 1559–1580. https://doi.org/10.1029/2017GC007271

Received 4 OCT 2017
Accepted 29 MAR 2018
Accepted article online 17 APR 2018
Published online 16 MAY 2018

Abstract We present a global compilation of paleomagnetic data spanning the past 100 ka. Sediment data comprise 61,687 declinations, 70,936 inclinations, and 69,596 relative paleointensities. Many sites are located in the northern Atlantic and western Pacific, with approximately twice as many data from the Northern Hemisphere as from the Southern Hemisphere. The 14,954 volcanic and archeomagnetic data are sparse, especially in the Southern Hemisphere. Directional and intensity information are aggregated under the paleosecular variation (PSV) index to assess occurrence of excursions over the past 100 ka. The Laschamp excursion (~41 ka) is clearly defined across globally distributed sediment records with an average duration of 1,300 years. Regional stacks obtained using bootstrap resampling show a more pronounced Laschamp excursion in the Northern Hemisphere than in the Southern, and in the Atlantic Hemisphere compared with the Pacific. No anomalous indices occurred around the Mono Lake excursion or other periods in the bootstrap curves. This may result from low sedimentation rates, discrepancies in age scales, large age errors, and/or the lack of global character of any transitional events. These data and associated new uncertainty estimates for the sediment records provide a good foundation for global, time-dependent, spherical harmonic field modeling for the past 100 ka.

1. Introduction

The geomagnetic field measured at Earth's surface includes contributions from sources both internal and external to the planet. The main geomagnetic field, which is generated by magnetohydrodynamic processes in Earth's liquid iron outer core, exhibits spatial and temporal variations that can be observed directly over the past 400 years (e.g., Jackson et al., 2000) and indirectly over geological timescales via remanent magnetization in crustal rocks and sediments. Paleomagnetic data obtained from sediments and lava flows spanning the past 100 thousand years (Late Quaternary) enable the evolution of the geomagnetic field to be reconstructed on millennial timescales.

Of particular interest during the 0–100 ka interval is that this stable period of normal polarity has been interrupted by multiple geomagnetic excursions: Hilina Pali, Mono Lake, Laschamp, Norwegian-Greenland Sea, and Skálamælifell or post-Blake excursion (e.g., Laj & Channell, 2015; Singer, 2014). Though they are recorded in one or more locations, there is an ongoing discussion about the global nature and robustness of these geomagnetic events. The best documented is the Laschamp excursion (~41 ka), first identified in the Laschamp and Olby lava flows from La Chaine des Puys (Massif Central, France) (Bonhommet & Zähringer, 1969) and later described in lava flows from Iceland (e.g., Kristjansson & Gudmundsson, 1980; Levi et al., 1990) and New Zealand (Cassata et al., 2008). The Mono Lake/Auckland excursion is another younger event with a range of age estimates, peaking around ~32 ka (Benson et al., 2003; Cassata et al., 2008; Denham & Cox, 1971; Kissel et al., 2011). There are sediment magnetic records that exhibit two successive paleointensity lows dated at 32–34 ka (Mono Lake) and 41 ka (Laschamp) (e.g., Channell, 2006; Lund et al., 2005; Nowaczyk et al., 2013; Singer et al., 2009).

The past geomagnetic field has been studied regionally and globally on different time-scales. For example, a suite of models covering the Holocene exists: CALS models (Constable et al., 2016; Korte & Constable, 2003, 2005, 2011; Korte et al., 2009, 2011), A_FM, ASD_FM, and ASDI_FM (Licht et al., 2013), pfm9k (Nilsson et al., 2014), SHA.DIF.14k (Pavón-Carrasco et al., 2014), and HFM models (Constable et al., 2016; Panovska

et al., 2015). Time-averaged field models have been constructed for normal and reversed polarity periods for the past 5 Myr (Johnson & Constable, 1995, 1997; Kelly & Gubbins, 1997) and a time-dependent model of the 0–2 Myr paleomagnetic axial dipole moment PADM2M is available (Ziegler et al., 2011). Paleointensity variations have been described using global stacks including GLOPIS-75 (Laj et al., 2004), Sint-200, Sint-800 and Sint-2000 (Guyodo & Valet, 1996, 1999; Valet et al., 2005), and PISO-1500 (Channell et al., 2009) constructed by correlating paleointensity and oxygen isotope records. Regional paleointensity stacks have been generated for the North Atlantic (NAPIS-75) (Laj et al., 2000), South Atlantic (SAPIS) (Stoner et al., 2002), western equatorial Pacific (EPAPIS) (Yamazaki & Oda, 2005), and northwest Pacific (NOPAPIS-250) (Yamamoto et al., 2007).

One of the requirements for modeling paleofield behavior is measurements of the full paleomagnetic vector field, i.e., both direction and intensity. Intensive efforts have been made to compile all available paleomagnetic, archeomagnetic, and volcanic data on different timescales. The most recent database, HISTMAG, combines the archeomagnetic and volcanic records from the past 50 ka with historical data covering the past 500 years (Arneitz et al., 2017b). The GEOMAGIA50 database (Brown et al., 2015a; Donadini et al., 2009; Korhonen et al., 2008) comprises data from archaeological and igneous sources with ages less than 50 ka. This database has been expanded to accommodate sediment records as well (Brown et al., 2015b). Sediment data contributing to the Global Paleointensity Stack for the past 75 ka (GLOPIS-75; Laj et al., 2004) and PINT absolute paleointensity database (Biggin et al., 2009; Biggin & Paterson, 2014) cover periods older than 50 ka. For older ages, the PSV10 database contains paleodirections and paleointensities for the last 10 Ma (Cromwell et al., 2018). Tauxe and Yamazaki (2007) compiled the SEDPI06 collection of relative paleointensities (RPI) from globally distributed sediment cores. A significant number of records are also available from the PANGAEA (Diepenbroek et al., 2002) and the Ocean Drilling Program (ODP) and International Ocean Discovery Program (IODP) databases (http://www-odp.tamu.edu/database/). In recent years, there have been a number of new corings (e.g., Collins et al., 2012; Channell et al., 2012a, 2012b; Lisé-Pronovost et al., 2013; Nilsson et al., 2011; Nowaczyk et al., 2012; Xiao et al., 2016; Yang et al., 2012) that significantly enhance global data coverage. These studies provide high-resolution paleointensity and directional records that will facilitate the construction of global, time-dependent models of the 0–100 ka geomagnetic field.

A long-standing problem in the inversion of paleomagnetic data is assigning realistic and consistent uncertainty estimates. Various strategies have been employed to estimate uncertainties enabling the use of paleomagnetic data in constructing temporally continuous harmonic models of the paleomagnetic field. The most frequently reported values for directional data are 95% confidence circle about the mean (α_{95}) (Fisher, 1953), and the standard deviation (σ_F) of the intensity. The α_{95} values can be converted to standard deviation errors in declination and inclination (e.g., Donadini et al., 2009). For Holocene field models, e.g., CALS3k.3 or CALS10k.1 (Donadini et al., 2009; Korte et al., 2009, 2011), minimum uncertainties were assigned for directional and intensity data. Other models, e.g., Licht et al. (2013) used the original error estimates (when available) and added a modeling error to the data uncertainty. By resampling the data set across temporal intervals, Nilsson et al. (2014) obtained uncertainty estimates based on the dispersion of the data within each uniform temporal bin. They also used minimum uncertainties for the sedimentary records when the method resulted in unsuitable estimates. The approach we will adopt in the current work was developed by Panovska et al. (2012), who used a cross-validation technique combined with smoothing spline analysis to systematically derive uncertainty estimates and measures of temporal smoothing for individual Holocene sediment magnetic records.

Studying the long-term temporal and spatial complexity of the field over the past 100 ka is of interest for understanding the driving mechanisms of the geodynamo. A new paleosecular variation (PSV) index has been introduced by Panovska and Constable (2017) as a tool for assessing the internal geomagnetic field complexity and variability and distinguishing between stable and transitional field behavior on both local and regional scales. Panovska and Constable (2017) applied this index to modern and historical geomagnetic field models and found clear regional differences in the PSV activity with highest values over the Southern Atlantic Hemisphere. Their results were consistent with the new regional paleomagnetic axial dipole moment models derived by Ziegler and Constable (2015), which showed systematic differences when records from specific latitude and longitude bands are used to constrain the models over the interval 0–300 ka.

The data compilation presented in this paper is the first step toward building a global, time-dependent, geomagnetic field model for the past 100 ka. The paper describes the data sources used for the

compilation, the geographical, and temporal distribution of the data (section 2), the methods used to date sediments and volcanic rocks and the limitations on the chronology (section 3), new uncertainty estimates for paleomagnetic records from sediments (section 4), comparison of paleointensity records with available paleomagnetic models and RPI stacks (section 5), and an analysis of PSV for the past 100 ka using the PSV index, highlighting the character of the index during geomagnetic excursions (section 6).

2. Data

2.1. Sources

We compile paleomagnetic data from (1) lake and marine sediments; (2) volcanic rocks; and (3) archaeological materials. The sediment data set comprises 116 declination, 129 inclination, and 157 RPI records. The initial source for sediment RPI records was the SEDPI06 compilation of Tauxe and Yamazaki (2007). All 88 RPI records from SEDPI06 covering the past 100 ka are included. Forty-three of these records have inclination but only 38 have declination components. Tauxe and Yamazaki (2007) recalculated the ages of some of the SEDPI06 records (eight of which are used in this compilation) by linear rescaling of their ages to the date for the Matuyama-Brunhes boundary given in Cande and Kent (1995) and we retained the adjusted chronologies. Furthermore, the data compilation is expanded with 60 RPI, 66 inclination, and 60 declination sediment records, most provided by the authors of the individual studies. In a few cases data were available online at MagIC website https://www.earthref.org/MagIC, GEOMAGIA50.v3 (sediment part) (Brown et al., 2015b), Pangaea (Diepenbroek et al., 2002), and ODP/IODP databases. Sediment records from the Holocene compilation of Korte et al. (2011) which exceed 10 ka in length have also been included (9 RPI, 20 inclination, and 18 declination records). They significantly improve the spatial distribution especially over the continents for the first 10 ka of the compilation.

Archeomagnetic and volcanic data spanning 0–50 ka were drawn from the GEOMAGIA50 database (download date 30 April 2015). To cover the period from 50 to 100 ka, we selected 313 data points from an early version of the global 0–10 Ma PSV10 data set (Cromwell et al., 2018), which included volcanic data published through to the end of 2013. Directional data have been selected from high-quality sites defined with the following selection criteria in Cromwell et al. (2018): mean directions determined from four or more specimens that were fully demagnetized; had their individual characteristic remanence directions derived using principal component analysis (Kirschvink, 1980); and have Fisher precision parameters $k \geq 50$. We only included data with absolute ages derived from radiometric dating methods and excluded data where the dates were given as age intervals with minimum and maximum age values. Regarding the uncertainties, all selected directional data from the PSV10 database have associated α_{95} (in the range of 1.4° to 10.1° with a median of 4.2°), but only 15% of the intensity data are accompanied by uncertainty values (range: 0.2 μT to 12.7 μT, a median of 5 μT). 64.1% of the GEOMAGIA50 directional data have α_{95} (a median of 2.9°) and 48.8% of the intensities come with an uncertainty estimate (a median of 2.5 μT). Both the data with no uncertainty and with small uncertainty need to be assigned a minimum error. The threshold values for the Holocene models were set to α_{95} of 4.3° and intensity uncertainty of 5 μT (Donadini et al., 2009). These were estimated by comparing the data with the *gufm1* model predictions for the historical period (Korte et al., 2005) and later RMS deviations for directions were converted to α_{95} values. Recently, Arneitz et al. (2017a) introduced a new approach for analyzing archeomagnetic and volcanic data by comparison with historical records and applying temporal and spatial mismatches with weighting functions. Their posteriori estimates imply that reported measurement errors are underestimated.

2.2. Temporal and Spatial Distribution

Data are mainly concentrated in northern midlatitudes, although about 30% come from the Southern Hemisphere. The numbers of data are given in Table 1, and the spatial distributions in Figure 1, where we see that the North Atlantic and West Pacific both have relatively high concentrations. Temporal distributions show that the number of sediment data increases toward more recent times with better coverage for the past 50 ka (Figure 2). The total number of sediment intensity data is slightly higher than directional data in contrast to the Holocene sediment compilation which has more directional than intensity data (Korte et al., 2005, 2011). The Laschamp excursion at 41 ka is well represented by both directional and intensity sediment data. Supporting information Tables S1 and S2 list the names, location, coordinates, mean sedimentation rate, age range, dating methods, and references for the individual sediment records. All sediment

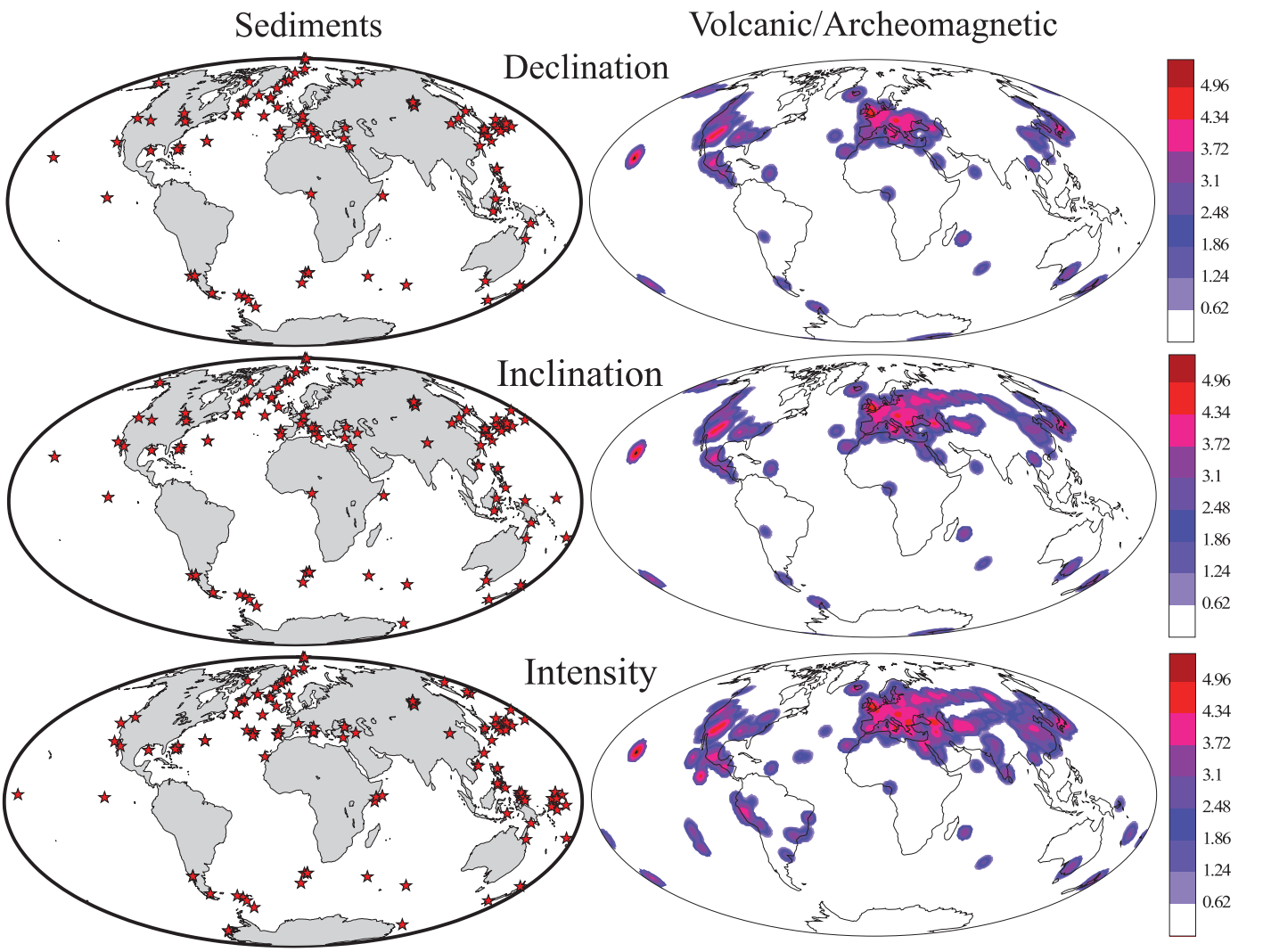

Figure 1. Locations of the global compilation of paleomagnetic and archeomagnetic data. On the left, locations of sediment records are noted with stars, while on the right distributions of volcanic and archeomagnetic data are plotted as a probability distribution function on a log scale. Red (purple) values show areas with a high (low) concentration of data. White areas have no data.

records are available from the following link https://earthref.org/ERDA/2223/. Archeomagnetic and volcanic data constitute less than 10% of the total data compilation. Their number is especially small in the Southern Hemisphere (Figure 1). In general, archeomagnetic and volcanic data have ages <10 ka. New data that

Table 1
Evaluation of Compiled Data Covering the Past 100 ka From Sediment Magnetic Records and Archeomagnetic/Lava Flows

Hemisphere	Component	Sediment	Archeomag./lava (GEOMAGIA50)	Lava flows (PSV10)	All
Northern Hemisphere	Declination	40,982 (92 records)	3759	56	44,797
	Inclination	50,004 (103 records)	5441	56	55,501
	Intensity	49,634 (125 records)	4835	3	54,472
	Total	140,620	14,035	115	154,770
Southern Hemisphere	Declination	20,705 (24 records)	129	78	20,912
	Inclination	20,932 (26 records)	129	78	21,139
	Intensity	19,962 (32 records)	348	42	20,352
	Total	61,599	606	198	62,403
Sum, global		202,219	14,641	313	217,173

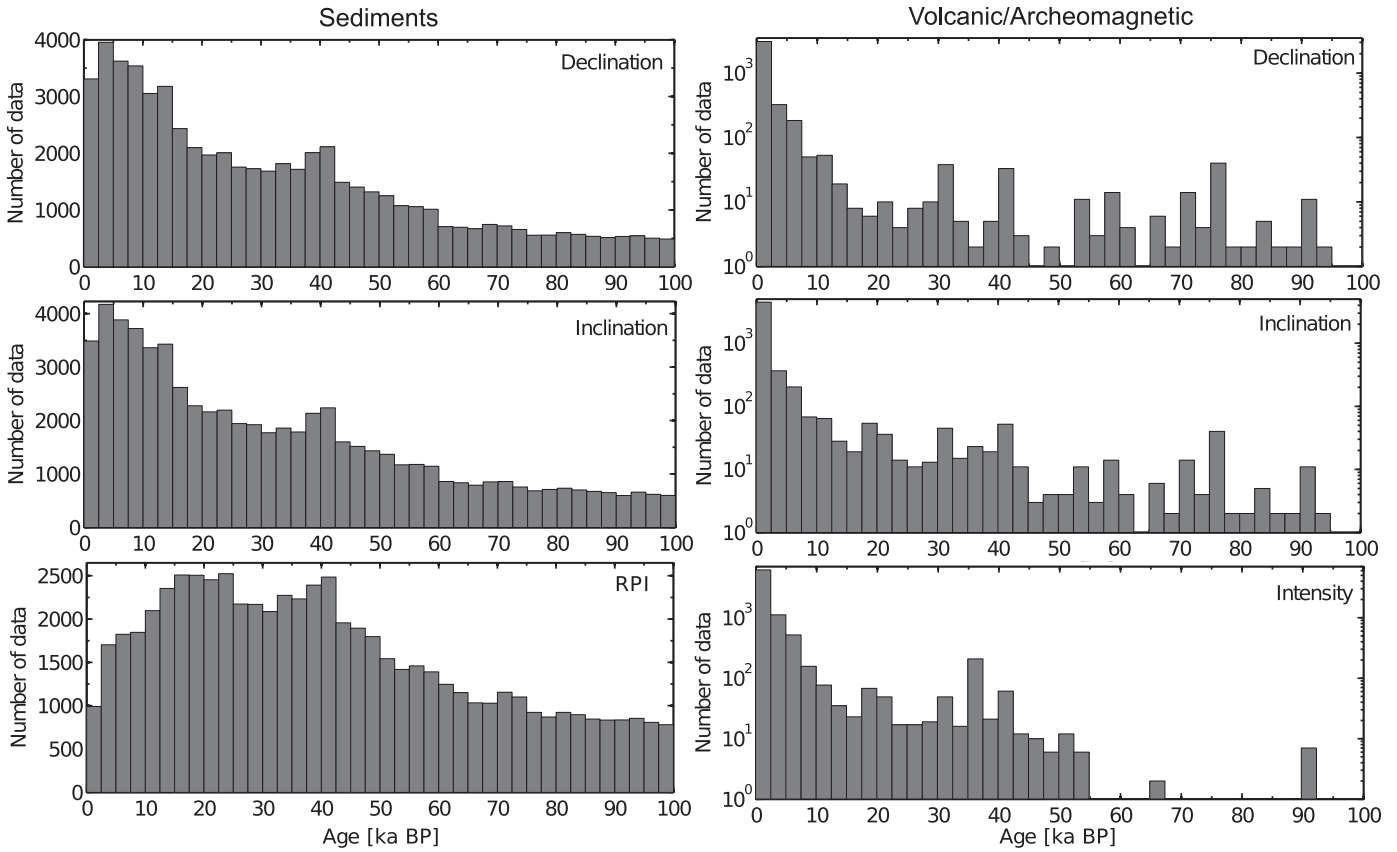

Figure 2. Histograms of temporal distributions of declination, inclination, and intensity of sediment magnetic records (left) and volcanic and archeomagnetic data (right). Note the logarithmic vertical axis scale for the volcanic/archeomagnetic data.

would be useful for this and future modeling efforts should be uploaded to the publicly accessible MagIC database at https://www.earthref.org/MagIC.

3. Geochronology

3.1. Dating Methods

An essential factor for studying the past geomagnetic field evolution is the provision of an accurate and high-resolution chronology for the various records. This also provides the basis for estimating sedimentation rates and temporal resolution of the observations. A variety of dating methods has been used to assign a timescale to the paleomagnetic sediment records and the distribution across the data set is shown in Figure 3a. Radiocarbon (^{14}C) dating is the most commonly used geochronological method. ^{14}C dating is limited to samples that are younger than 50 ka. Many factors influence the resulting radiocarbon ages (see review by Björck & Wohlfarth, 2001) including the calibration of ^{14}C ages to calendar years. The ^{14}C calibration is more certain for the past 14 ka where calibration is based on tree-ring records (Hua et al., 2009), but advances have been made to extend radiocarbon calibration back to 50 ka (e.g., IntCal13; Reimer et al., 2013). The uncertainty in the calibrated age is generally larger than the uncertainty in the radiocarbon age, and it depends on the time period of the calibration curve. Recently, Muscheler et al. (2014) connected a ^{14}C tree-ring chronology to ice-core ^{10}Be records prior to the midpoint of the Laschamp excursion. The results suggest that the ^{14}C calibration curve IntCal13 yields calendar ages that are too old by about 1,200 years for this period. This would have consequences for the timing of the Laschamp Excursion recorded in sediments solely based on calibrated radiocarbon ages.

Oxygen isotope (δ^{18}O) dating is obtained when measurements of oxygen isotopes in planktic or/and benthic foraminifera are correlated to reference curves of oxygen isotope variations, such as SPECMAP (Imbrie et al., 1984; Martinson et al., 1987), GRIP (Dansgaard et al., 1993; GRIP members, 1993), GISP2 (Grootes &

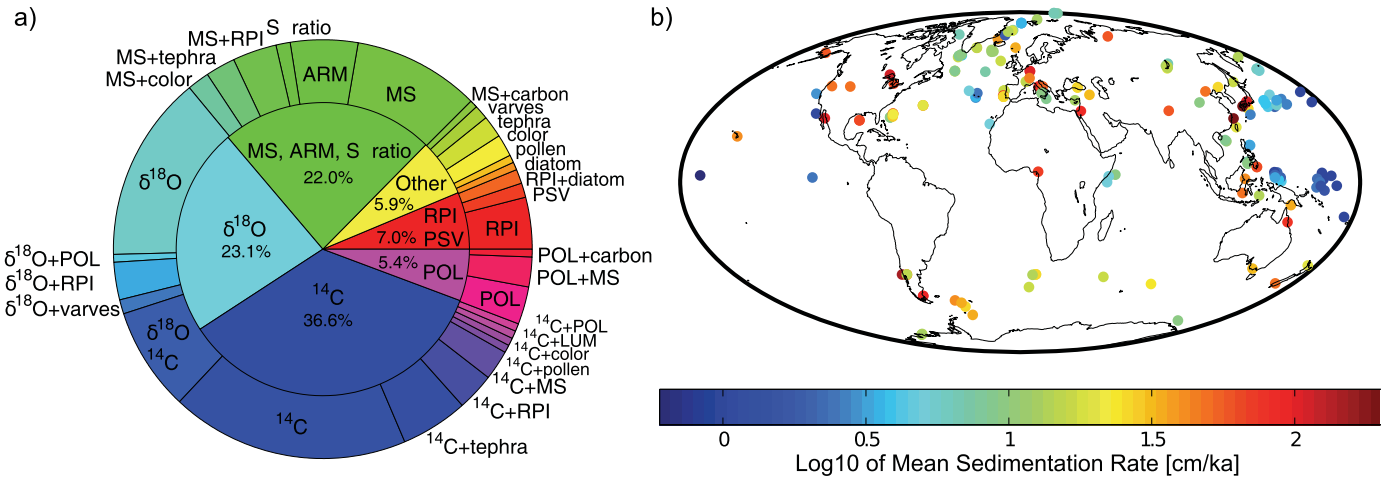

Figure 3. (a) Pie chart presenting the different dating techniques used for age determinations of the global magnetic sediment records. Abbreviations: δ^{18}O: oxygen isotope stratigraphy; ^{14}C: radiocarbon; POL: polarity stratigraphy; RPI: relative paleointensity; PSV: correlation of paleosecular variation; MS: correlation of magnetic susceptibility; ARM: correlation of anhysteretic remanent magnetization; S-ratio: correlation of S-ratio; pollen: pollen stratigraphy; color: correlation of color (light reflectance); carbon: correlation of calcium carbonate; diatom: diatom abundance stratigraphy; LUM: thermoluminescence. Methods that appear only in single records as additional tie-points (U-Th, ^{230}Th, δ^{13}C, gamma ray count) have been left out of the figure for the sake of simplicity. (b) Map of mean sedimentation rate in cm/ka of magnetic sediment records compiled in this study. The color corresponds to the logarithm of sedimentation rate. The highest sedimentation rate estimated for Beppu Bay, Japan: 200 cm/ka (log10(200) = 2.3 on the plot), the lowest in the Central Pacific Basin, core p226: 0.6 cm/ka (−0.2) and the median sedimentation rate is 13 cm/ka (1.1). All values are listed in supporting information Table S1.

Stuiver, 1997; Meese et al., 1997; Stuiver & Grootes, 2000), GICC05 (Andersen et al., 2006; Svensson et al., 2006, 2008), and LR04 (Lisiecki & Raymo, 2005). Oxygen isotope signals from the undated records can also be correlated to independently dated oxygen isotope records, such as radiocarbon dated sediments (e.g., Channell et al., 2000) or magnetic concentration parameters, for example magnetic susceptibility, anhysteretic remanent magnetization (ARM), and saturation isothermal remanent magnetization (SIRM) (e.g., Nowaczyk et al., 2012). The resolution of δ^{18}O scales varies from 3 to 5 ka for SPECMAP, 1 ka for LR04 (time interval 0–0.6 Ma) to several years for GISP2 and GICC05 δ^{18}O records (Andersen et al., 2006; Stuiver & Grootes, 2000). It is worth mentioning that these reference curves are not always compatible with each other. For instance, Obrochta et al. (2014) reported a maximum of a few thousand years difference between the GISP2 and GICC05 chronologies.

Varve counting is possible in laminated sediments, i.e., sediments that record annual depositional cycles, for example in Eiffel Maars of Germany (Brown, 1991; Stockhausen, 1998) or Fennoscandian lakes (Snowball et al., 2007). The main advantage of the varve chronology is that in uniform and complete sedimentation environments varves have the potential to provide dating with a resolution of 1 year.

Correlation based on physical (silica, carbon, light reflectance signal, color) or magnetic properties (magnetic susceptibility, ARM, SIRM, S-ratio) is also used to transfer the age scale of one dated core to parallel cores without available ages (e.g., su92-17 (Lehman et al., 1996), NGC65 (Yamazaki, 1999), 1062B (Bourne et al., 2012), and CGC12 (Yamamoto et al., 2007)). A significant number of the sediment records have age models improved with additional independent dating points (tephra, varves, pollen, color, carbon). In some cases, the age-models have been assigned/adjusted with correlation based on paleomagnetic data (PSV and RPI) or model predictions, assuming that the field changes at the two locations occurred at the same time within the temporal resolution of the records, but these records are not suitable for geomagnetic field modeling.

Paleomagnetic data from the PSV10 database between 50 and 100 ka have been dated using K-Ar dating (37.3% of the data), Ar-Ar dating (11.9%), or through stratigraphy (50.8%). Chronological methods for the GEOMAGIA50 data are discussed in more detail in Brown et al. (2015a). About 26% of GEOMAGIA50 data have no metadata for the dating method making it hard to determine reliability of age information. The highest percentage (35%) of data have ages assigned by archeological methods.

Various geochronological methods are associated with a wide range of age uncertainties, reported in the literature as a standard deviation or standard error on the measurement, but uncertainties are often unavailable or unverifiable. Archeomagnetic and volcanic data in GEOMAGIA50 have age uncertainties with a median of 50 years (interquartile range of 10–130 years), while PSV10 lava flow data have a median of 5 ka (interquartile range from 3 to 10 ka). These errors are also important and should be considered when archeomagnetic and lava flows data are used to constrain a geomagnetic field model.

3.2. Sedimentation Rate, Data Resolution, and Lock-in Depth

For sediments there are several factors that need to be considered when determining the accuracy and resolution of the paleomagnetic records. These include sedimentation rate, lock-in depth, and smoothing associated with remanence acquisition, and whether the measurements are made on discrete samples or on U-channels with a pass through magnetometer.

The average sedimentation rates of the paleomagnetic records are plotted in Figure 3b. If the sedimentation rate was not reported in the original publication, then we calculated the mean rate using published age-depth models. Although all regions show a range of sedimentation rates, the Pacific is the region with lowest overall rates. Southern Ocean records have intermediate rates, and continental lakes have the highest rates. ODP 1233, offshore Chile (Lund et al., 2006a), MD06–3040, East China Sea (Zheng et al., 2014), and Beppu Bay, Japan (Ohno et al., 1991) are notable outliers with exceptionally high mean rates, 150.0, 194, and 200 cm/ka, respectively. The remainder has accumulation rates between 0.6 and 108.2 cm/ka. 45% of records have mean rates $<$10 cm/ka, 42% are in the range 10–50 cm/ka, 10% in the range 50–100 cm/ka, and 3% have rates $>$100 cm/ka.

The wide range of sedimentation rates may result in different levels of smoothing of the paleomagnetic signal recorded by the sediments. A post depositional remanent magnetization modeling of Roberts and Winklhofer (2004) suggested a minimum sedimentation rate of 10 cm/ka is needed to consistently detect geomagnetic excursions in sediment magnetic records. The actual resolution will of course depend on the sampling density and whether discrete or u-channel samples are used, for example discrete samples every 2.5 cm can do no better than a 250 year resolution at a sedimentation rate of 10 cm/ka, and the actual assessment of resolution can be somewhat difficult. In a recent study, Ziegler and Constable (2015) tested the influence of sedimentation rate on regional axial dipole moment reconstructions. Their results showed that not all the regional differences in variance can be assigned to variable sedimentation rates across records.

Our sediment compilation includes data from both discrete samples and u-channels. About one third of sediment data are obtained with u-channel sampling. Despite the advantage of much faster measurement and less sediment deformation, discrete sampling is preferable because u-channel data are not independent but are smoothed over the width of the instrument response function. Numerous studies (Constable & Parker, 1991; Dodson et al., 1974; Jackson et al., 2010; Oda et al., 2016; Oda & Shibuya, 1996; Parker & Gee, 2002; Roberts, 2006) have invoked deconvolution as a means to partially mitigate these effects, but there are complications with the u-channel data related to end effects and interference between orthogonal magnetometer pick-up coils. A study by Guyodo et al. (2002) on ODP 1090 sediments suggested that deconvolution can produce higher resolution records comparable to discrete sampling. Roberts (2006) discussed the pros and cons of long-core magnetic data and synthesized recommendations for avoiding the limitations of these measurements, including correction of negative response functions, measuring samples with geometrically uniform cross-section along the central line of the magnetometer, use of numerical deconvolution approaches, analysis of cores deposited at high sedimentation rates ($>$10 cm/ka), and use of sensors with a similar response function for measuring magnetic susceptibility and u-channel magnetometer to ensure data comparability. The impact of sensor alignment and cross-talk can be significant (Parker & Gee, 2002) and end effects remain a significant problem for which there is so far no practical solution.

Sediments record the paleomagnetic field through the acquisition of a detrital (depositional or post depositional) remanent magnetization (e.g., Griffiths, 1955; Irving & Major, 1964; Johnson et al., 1948; King, 1955; Tauxe, 2002). Estimates of the depth over which magnetization gets locked in sediments vary, ranging from $\sim$1 to 25 cm (Boudreau, 1994; Channell & Guyodo, 2004; Egli & Zhao, 2015; Hyodo, 1984; Lund & Keigwin, 1994; Roberts & Winklhofer, 2004; Stockhausen, 1998; Suganuma et al., 2011; Yamazaki, 1984). Tauxe et al. (2006) argued that the evidence for significant (deep) lock-in depth in marine sediments is weak based on

natural sediments as well as laboratory experiments. Recently, Egli and Zhao (2015) showed that lock-in functions depend on the mixing regimes. Small lock-in depths (~1 cm) are characteristic of pelagic sediments with slow mixing regime and shallow mixed layers, while rapid mixing regimes exhibit deep lock-in depths (~20 cm). Here we simply note that the impacts of delayed lock in are twofold: there is likely to be a temporal offset between chronological age and magnetization age, and sedimentation processes produce a convolution of the instantaneous magnetic signal with a filter that is dependent on the particular sedimentation process.

4. Uncertainty Estimates and Smoothing Time for Sediments

We have derived new uncertainty estimates for paleomagnetic records obtained from sediments covering the past 100 ka. We follow the methods of Panovska et al. (2012) that have been previously used to analyze paleomagnetic records from Holocene sediments. Smoothing splines are fit to individual time series and used to investigate the random variability present in each record. The root mean square residuals of the fit provide a measure of uncertainty within each record. For declination and inclination, this is measured in degrees, providing a generally reliable method to evaluate absolute uncertainties and record quality. RPI records are produced using several different normalizations, yielding a wide range of uncalibrated values that cannot be compared directly. To allow a global comparison of overall quality, each RPI record is scaled by the standard deviation derived from all values in the series and this is referred to as standardized RPI (see Panovska et al., 2012, equation (11)).

An example of this analysis applied to a declination record from Western Philippine Sea, MD97–2143 (Horng et al., 2003) is shown in Figure 4. Plots with the spline fit analysis for all records are available online from the EarthRef Digital Archive (ERDA) at http://earthref.org/ERDA/1893/. For the smoothing spline construction, we used cubic B-splines (De Boor, 2001) and a regular array of knot points with fixed 100 year spacing for most records and 50 years for the shorter Holocene sediment records. The degree of smoothing depends on the parameter λ (Figure 4e) and is determined with the cross validation (CV) method (Green & Silverman, 1994): it provides a tradeoff between data misfit and temporal complexity and allows estimation of an average smoothing time. This estimate is characteristic of the average kernel function acting as a temporal smoother across the time series, and expresses the effects of sedimentation rate, data resolution, and locking depth (e.g., Figure 4f). A lower limit is set for the smoothing time, here called the threshold smoothing time, calculated using the mean sedimentation rate and an assumed lock-in depth of 3 cm (see Panovska et al., 2012, equation (1)). The assumed lock-in depth is not a strong constraint in our analysis. More details and examples of the effect of lock-in depth are given in supporting information Figures S1 and S2. For 77% of the records in this compilation, the smoothing time is evaluated by the CV method, while for the remaining records it was set at the threshold. Due to the presence of large outliers in some records, we recalculated the spline fits after rejecting data lying further than three standard deviations from the initial spline fit. This affected 64% of the records with an average of nine data points rejected per record. An example of the effect of data rejection is presented in supporting information Figure S3.

The standard deviation (sigma2, Figure 4) is estimated from the scatter of the data about the spline fit. For some smoothed records (not available in the original form) and data from u-channels, the method yielded unrealistically small random uncertainties. This is a result of the closeness of the spline fit to the smooth data. The median standard deviation is 15.2° for declination (IQR—interquartile range: 8.4°–31.2°), 5.8° for inclination (IQR: 3.2°–8.2°), and 0.4 for standardized RPI (IQR: 0.2–0.6). The latter can be converted to absolute values (in μT) by multiplying with the standard deviation (to restandardize) and calibration factor of each RPI record. One way of getting calibration factors is by comparing the RPI with absolute intensity values and calculating the median ratio of absolute to relative paleointensities (Korte & Constable, 2006). If the spline fit through the archeomagnetic and volcanic data (section 5) is used for calibration, absolute uncertainty estimates for the paleointensity show a median value of 4.7 μT (IQR: 3.0 μT to 7.9 μT). Histograms of the uncertainty estimates by component are plotted in Figure 5.

An important aspect of this analysis is the assessment of the temporal resolution through calculation of the smoothing time associated with each record. This smoothing time is obtained by inverting a delta function input at the data point locations using the same smoothing parameter used to create the spline fit (e.g., Parker, 1994). The effective resolving kernel diagnoses the amount of smoothing in the spline model. The

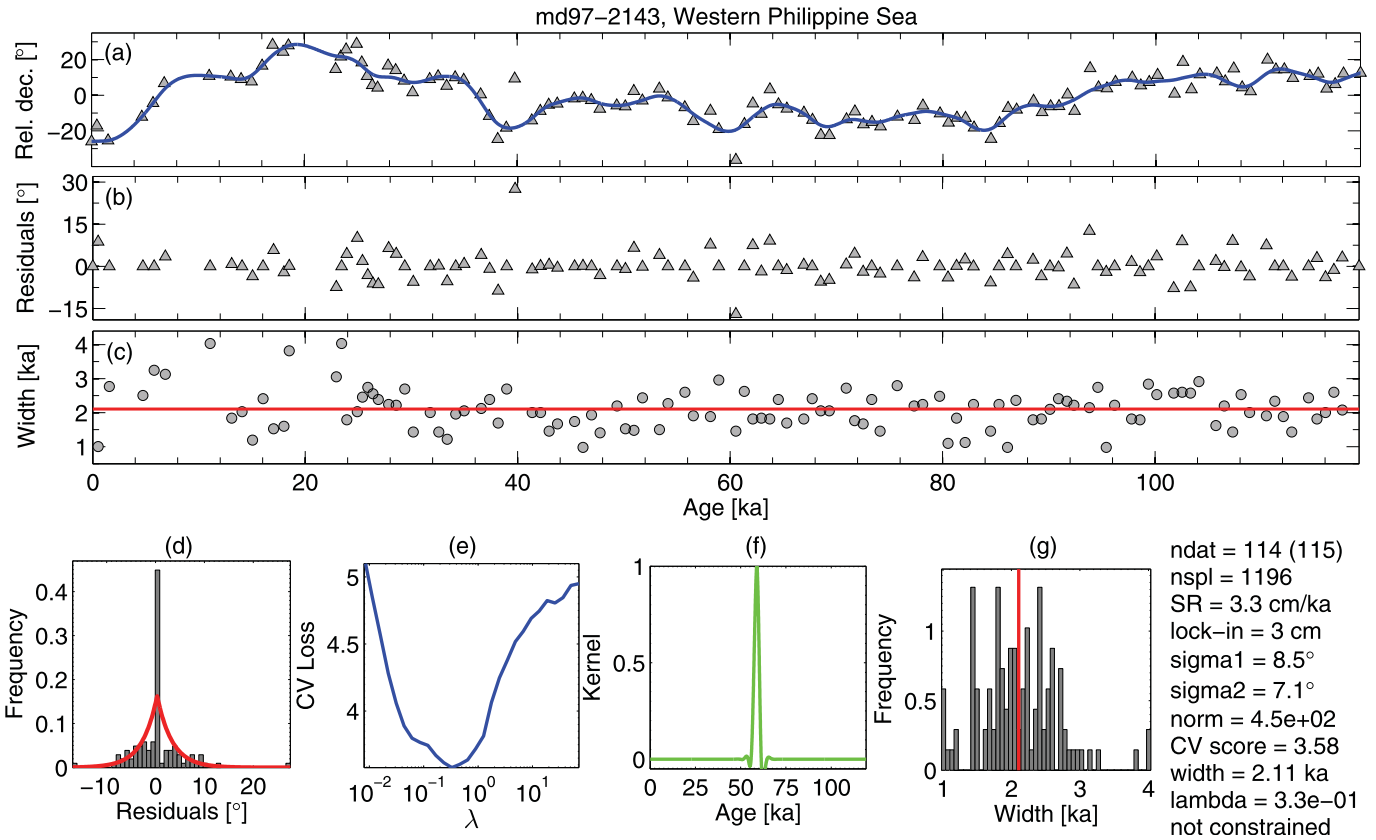

Figure 4. Example of the robust spline analysis of declination record from Western Philippine Sea MD97–2143 (Horng et al., 2003). (a) Data time series (gray triangles) and penalized least square spline fit (blue curve); (b) time series of residuals; and (c) time series of smoothing width. (d) Histogram of residuals (normalized to the unit area) is plotted with a Laplacian distribution (red curve) with mean and deviation calculated from the residuals. (e) Cross validation (CV) score as a function of the smoothing parameter λ (blue curve). The minimum of the CV score determines the choice of λ. The *x* axis on this subplot is given in logarithmic scale. (f) An example of kernel function estimated at the central point of the same record, which diagnoses the temporal resolution. The width refers to a full width at half maximum of this kernel function. (g) Histogram of estimated kernel widths and the mean value (red line). Information about the number of data (ndat), number of spline (nspl), mean sedimentation rate (SR), assumed lock-in depth, the L_1 measure of misfit (sigma1), the L_2 measure of misfit (sigma2 or σ_{rss}), the norm measuring the model roughness (norm), the value of the CV minimum (CV score), the mean width of the resolving kernel (width), the corresponding smoothing parameter λ (lambda), and the note if the smoothing parameter is constrained by the CV minimum function or by a-priori smoothing time are provided in the label.

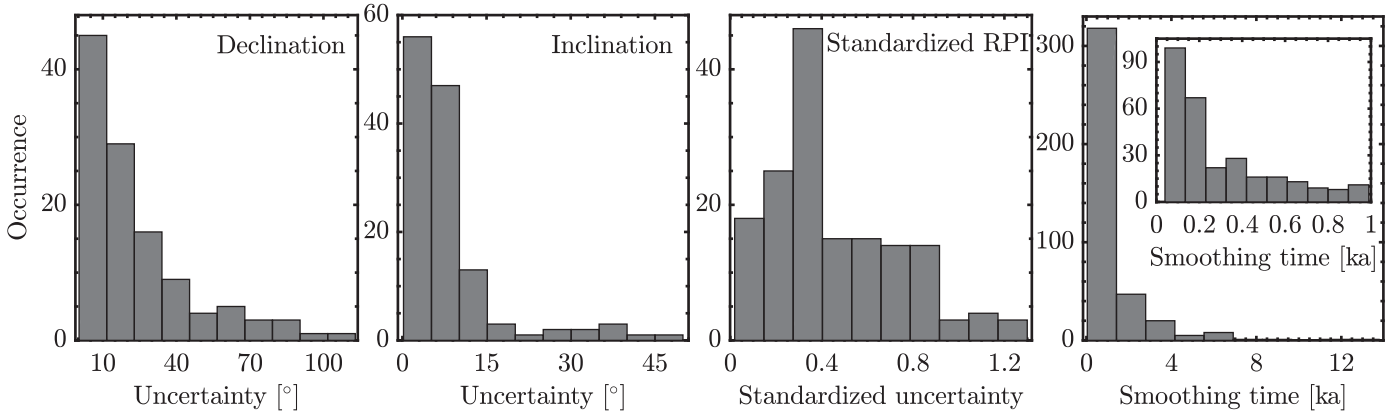

Figure 5. Histograms summarizing the total uncertainty estimates and smoothing times of the sediment records in the 100 ka global data compilation. Histograms are presented by component, whereas the histogram of the smoothing time combines the values for all three components. The inset presents a zoomed version of the smoothing time histogram for times <1 ka, the range in which more than 70% of the records lie.

width at half maximum height of the resolving kernel is calculated for every internal point and the average is reported in Figure 4 as "width." The smoothing times estimated from the spline modeling range from 40 years to 13.8 ka with a median value of 400 years (Figure 5). The strongest smoothing is observed at the Pacific NGC65 record (Yamazaki, 1999), where the low sedimentation rate limits the data resolution. Results for the uncertainty estimates and temporal resolutions for all sediment records are listed in supporting information Table S1.

5. Comparison of Compiled Data With Models and RPI Stacks

We have compared archeomagnetic and sediment data with predictions from available field models and RPI stacks, including PADM2M (Ziegler et al., 2011), IMOLE (Leonhardt et al., 2009), NAPIS-75 (Laj et al., 2000), SAPIS (Stoner et al., 2002), GLOPIS (Laj et al., 2004), PISO-1500 (Channell et al., 2009), NOPAPIS-250 (Yamamoto et al., 2007), Sint-800 (Guyodo & Valet, 1999), and Sint-2000 (Valet et al., 2005). Stacks of globally distributed relative palaeointensity records provide information regarding the evolution of the relative strength of the dipole field in the past as well as regional references for paleointensity-assisted stratigraphy. The disadvantage of stacking is that it reduces the resolution of the output compared with the input of individual records. Paleointensity stacks on a more local scale have been established as well, for instance the composite record of paleointensity from the Wilkes Land Basin off Antarctica (wega) (Macrì et al., 2005), the regional paleointensity stack from the West Caroline Basin (wcbstack) (Yamazaki et al., 2008), and the Baikal stack (Peck et al., 1996) among others.

Example comparisons of three sediment paleointensity records from North Atlantic (U1302-U1303, Channell et al., 2012a), South Atlantic (21-pc02, Stoner et al., 2002), and North Pacific (NGC108, Yamamoto et al., 2007) with existing models and RPI stacks are given in Figure 6. Long-term models and RPI stacks (Sint-2000, PISO-1500, PADM2M) have averaged out much of the high-frequency variability and they predict a smoothly varying field over the past 100 ka. Even though the stacks have similar trends, there are notable differences related to problems with inconsistent timescales, relatively large age uncertainties, imperfect global correlation when creating the stacks, and differences in the resolution of underlying data. Roberts et al. (2013) noted that the differences between stacks far exceed measurement uncertainties and errors due to the stacking process.

Records of the Laschamp excursion and/or an associated dipole low have been obtained from lacustrine (e.g., Demory et al., 2005) and marine sediments (e.g., Channell, 2006; Lund et al., 2005; Nowaczyk et al., 2012, 2013). The most recent chronological constraint for the age of the Laschamp excursion determined from the maximum VGP deviation is 41.1 ± 0.35 ka (Lascu et al., 2016), based on a combination of high-precision ^{230}Th dates and annual layer counting using confocal microscopy from a speleothem. All models and RPI stacks resolve the Laschamp excursion, but minima at 32–34 ka (associated with the Mono Lake excursion) and 65 ka are only present in the GLOPIS-75 and regional stacks NAPIS-75 and SAPIS. GLOPIS-75 exhibits some high-frequency features that are not observed in the other stacks. A possible cause of this inconsistency is that RPI stacks are created from a limited number of records, for instance, 17 RPI records in Sint-200, 33 records in Sint-800, 6 in NAPIS-75, 5 in SAPIS, 24 in GLOPIS-75, 13 in PISO-1500, 10 in Sint-2000, and 10 in NOPAPIS-250 stack. Usually, one core is selected as a reference for the age scale of the stack or age models have been refined with respect to the oxygen isotope reference curves SPECMAP (e.g., Sint-200 and Sint-800) or GISP2 (e.g., NAPIS-75). Different δ^{18}O reference curves result in additional differences in timescales (Obrochta et al., 2014) and these also contribute to discrepancies among the stacks.

Archeomagnetic and volcanic intensity data (presented as VADMs) are plotted in Figure 7 for comparison with global models and paleointensity stacks. A temporal bias in the data distribution is evident as most of the data come from the past 10 ka, whereas the coverage is very sparse for the rest, especially for the 50–100 ka period. The best-fitting VADM to GEOMAGIA50 data by Knudsen et al. (2008) is well constrained for the Holocene and agrees with our spline fit. The smoothing spline modeling technique with a 200 years knot spacing was applied to the data from GEOMAGIA50 and PSV10 databases. The spline fit shows relatively smooth variations due to the sparse data points in the older period and a strong mismatch with the RPI stacks between 40 and 60 ka. Therefore, it is important that the new geomagnetic field model be constrained by the combination of volcanic, archeomagnetic, and high-resolution sedimentary data.

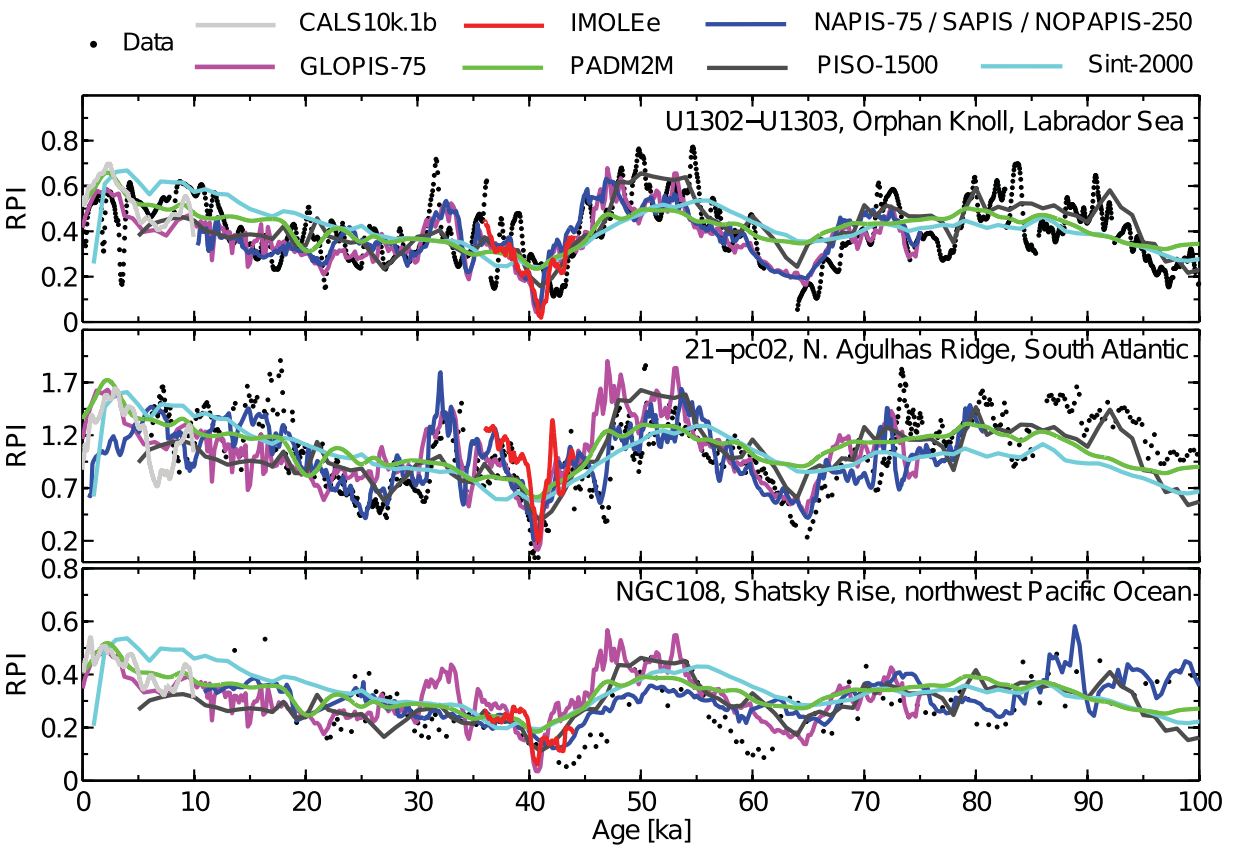

Figure 6. Three RPI sediment records that cover the past 100 ka are selected from different regions to show the comparison with existing paleomagnetic field models, and regional and global RPI stacks: U1302-U1303, North Atlantic (Channell et al., 2012a), 21-pc02, South Atlantic (Channell et al., 2000; Stoner et al., 2002), and NGC108, North Pacific (Yamamoto et al., 2007). Blue curves represent NAPIS-75 for the North Atlantic sediment record, SAPIS for the South Atlantic, and NOPAPIS-250 for the North Pacific record. For the purpose of plotting on one scale, all models and stacks are scaled to the sediment record RPI level.

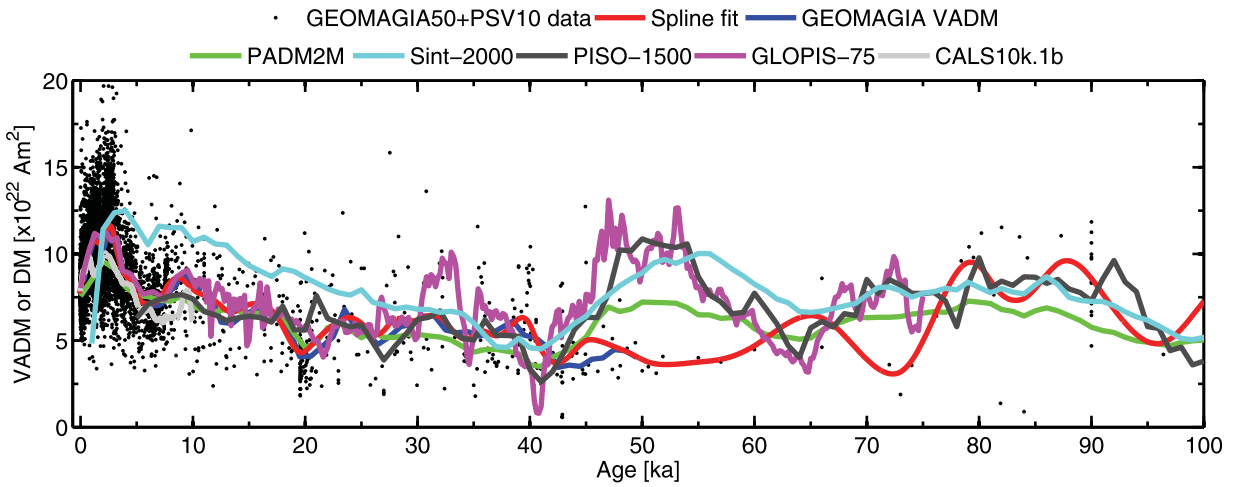

Figure 7. Distribution of virtual axial dipole moment (VADM) archeomagnetic and lava flow data from the GEOMAGIA50 (0–50 ka) and PSV10 database (data only from 50 to 100 ka). Global models and stacks are shown for comparisons: PADM2M model (Ziegler et al., 2011), Sint-2000 (Valet et al., 2005), PISO-1500 (Channell et al., 2009), GLOPIS-75 (Laj et al., 2004), and CALS10k.1b dipole moment (DM) (Korte et al., 2011). GEOMAGIA VADM represents variations in the geomagnetic dipole moment reconstructed by Knudsen et al. (2008). Note that the present GEOMAGIA50 data set is updated and different from the compilation used for the GEOMAGIA VADM. The red line is our spline fit to archeomagnetic VADM data over the last 100 ka. The spline fit predictions are used for calibration of all RPI sediment records. Note also the difference in resolution between the long-term models and stacks (PADM2M, Sint-2000, and PISO-1500) and GLOPIS-75.

6. PSV Activity Index and Geomagnetic Excursions

Panovska and Constable (2017) proposed the PSV index as a tool for characterizing variations in the geomagnetic field and for discriminating among PSV, excursions, and reversals. The index combines the virtual geomagnetic pole (VGP) latitude λ_p position and the virtual dipole moment, M, normalized to the present-day dipole moment M_0:

$$P_i(\lambda,\phi,t)=\frac{(\pi/2-|\lambda_p(\lambda,\phi,t)|)/\pi}{M(\lambda,\phi,t)/M_0} \quad (1)$$

Stable geomagnetic field, dominated by an axial dipole, as determined from modern and historical geomagnetic field models, exhibits values of $P_i \leq 0.3$. The conventional limit for identification of geomagnetic excursions, 45° VGP colatitude and dipole moment of 50% of the present-day value, would give a PSV index of 0.5. The standard deviation in P_i over time $\sigma_{P_i}(t)$ can be used to provide an overall measure of activity during any fixed time interval.

We computed the PSV index for all sediment records in the compilation and use it to illuminate geomagnetic field stability over the past 100 ka in global and regional (hemispherical) curves (Figure 8). We first calibrated the RPI data using a spline fit to all archeomagnetic and volcanic VADMs spanning the past 100 ka (Figure 7). The declination component is ignored for the calculation of the VGP latitude and $D = 0$ is used instead. (More details on the effect of this assumption can be found in Panovska and Constable (2017), but in general the effect is a slight underestimate in P_i at times of high PSV activity). A few examples of the PSV index for individual sediment paleomagnetic records are available in supporting information Figure S4. Sediment records manifest various levels of secular variation, especially at times when excursions occurred. The best recorded event is the Laschamp excursion with the highest indices estimated for the following calibrated sediment records: $P_i = 10.9$ at 41.3 ka in M72/5–22, Black Sea (Nowaczyk et al., 2012); $P_i = 9.0$ at 40.5 ka in ps2644-5, Iceland Basin (Laj et al., 2000); $P_i = 8.5$ at 40.5 ka in ODP 1089, South Atlantic (Stoner et al., 2003); $P_i = 7.6$ at 41.0 ka in JPC-14, North Atlantic (Lund et al., 2005); $P_i = 6.8$ at 40.9 ka in MD94–103,

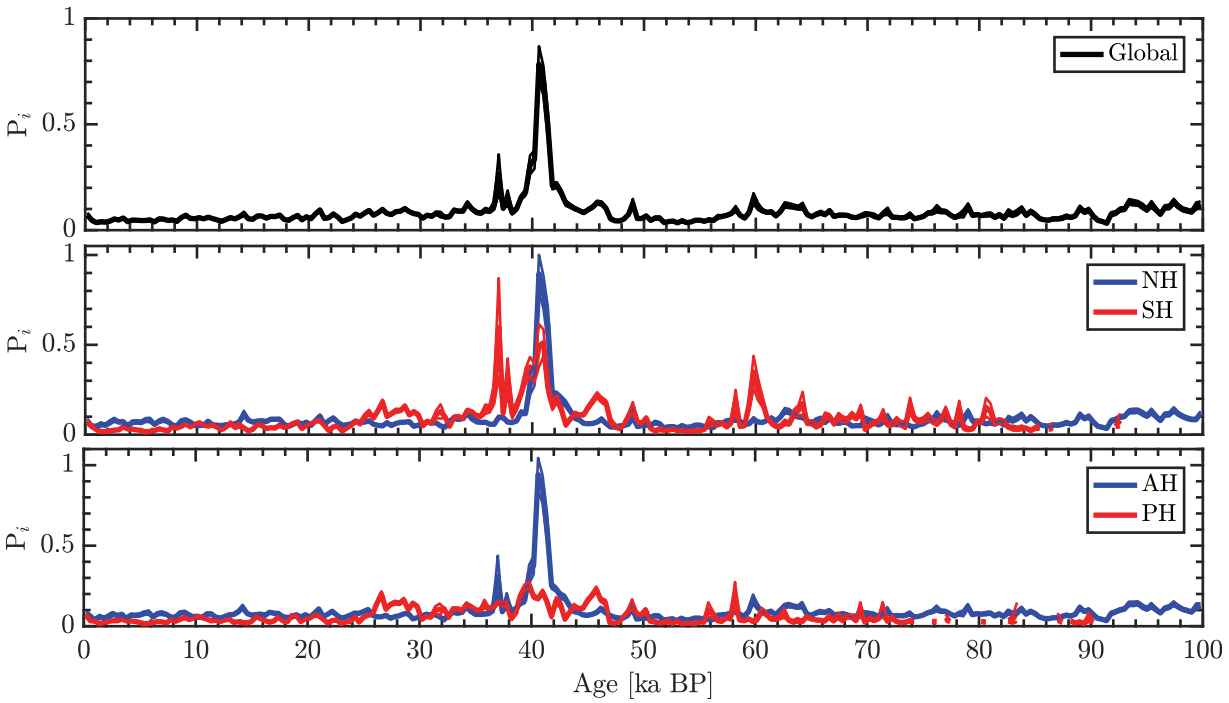

Figure 8. Summary of the PSV index for the sediment magnetic records compiled in this study (semi-dependent data set, see section 6 for details). The PSV index variations are averaged together globally and separately by hemispheres, Southern (SH) versus Northern (NH) and Atlantic (AH) versus Pacific (PH). For the purpose of stacking, 5,000 bootstrap resamplings are performed. For each resampled data set, a PSV index curve is estimated by averaging the data over 400 year time intervals—the size of the window is chosen based on the expected temporal resolution obtained from the spline analysis. Global and hemispherical stacks are presented with a mean value and one standard deviation from 5,000 bootstraps. Gaps in the curves appear for time intervals where no data are available.

Southern Indian Ocean (Mazaud et al., 2002); $P_i = 6.7$ at 39.9 ka in ODP 919, Irminger Basin (Channell, 2006); $P_i = 6.3$ at 40.8 ka in CH89-9P, North Atlantic (Lund et al., 2005); and $P_i = 5.2$ at 40.7 ka in MD02–2551, Gulf of Mexico (Laj et al., 2006). Peaks in the PSV index for the Mono Lake excursion, where recorded, are less than half the values of the Laschamp excursion. The ages of the PSV index maximum vary from one location to another which may be due to the main directional changes or intensity variations of the excursion occurring at different times (Brown & Korte, 2016) or to inherent age uncertainties in the sediment records. The absence of specific excursions in some sediment records could possibly be attributed to smoothing by the sedimentary remanence acquisition process and low sedimentation rates. However, no correlation between the mean sedimentation rates and nontransitional PSV indices is found (supporting information Figure S5). It is worth mentioning that a few records with low sedimentation rates (<10 cm/ka) have PSV indices larger than 0.5 during the Laschamp excursion: U1308 (Channell et al., 2008), MD97–2143 (Horng et al., 2003), ver98-1-14 (Demory et al., 2005), and ps1535-10 (Nowaczyk et al., 2003) (supporting information Table S3).

For the purpose of analyzing the PSV index variations of the sediment records, we categorized the data into three data sets: all, independent (whose timescales are independent of correlations based on paleointensities or paleodirections) and semi-dependent (contains the independent data set plus sediment records with independent age models which have been improved with tie points generally related to geomagnetic excursions). The results presented in this section are based on the semi-dependent data set that contains 135 RPI, 110 inclination, and 97 declination records (see supporting information Figure S6 for the spatial distribution of these data sets). We nominally divide the PSV index into Northern and Southern Hemispheres and by longitudes of 70°W and 110°E to approximate Atlantic/Pacific Hemispheres (with the exception of 1061B and 1061C (Bourne et al., 2013) and JPC-14 (Lund et al., 2005) from Blake Ridge, and MD02–2551 and MD02–2552 (Laj et al., 2006) from Gulf of Mexico which are assigned to the Atlantic Hemisphere). Furthermore, we calculated 5,000 individual bootstrap curves to estimate the standards error in P_i and the results are presented in Figure 8. Uncertainties in the magnetic components and ages are not used when generating the bootstrap samples. Globally averaged PSV index shows a very pronounced peak at 40.6 ka, a smaller peak at 37.0 ka, and a few time periods of insubstantial increased activity, some of which originate from individual records or locations. The peak associated with the Laschamp excursion has a value of 0.78 ± 0.08. Regional bootstrap curves have some considerable differences, especially during periods of increased indices. The Laschamp excursion is a dominant feature of the PSV index determined from Northern and Atlantic Hemisphere sediments. Only records from the Southern hemisphere exhibit the second peak at 37 ka in contrast to the Northern hemisphere where the paleomagnetic field is stable. In the Pacific Hemisphere, the period around the Laschamp excursion shows no excursional PSV indices and overall values are very low for the whole 100 ka. These findings are consistent with the results of Ziegler and Constable (2015), where excursions have been analyzed in terms of axial dipole moment minima in global and regional models. In their regional models, average Pacific VADM is higher than Atlantic, which in turn will contribute to lower P_i values. However, recent measurements of lavas from New Zealand show excursional paleodirections in ages between 46.3 and 42.7 ka (Ingham et al., 2017), and it is possible that low sedimentation rates of Pacific sediment cores is the reason for the absence of the Laschamp event in the Pacific Hemisphere.

The Mono Lake excursion is not visible in the PSV index stacks (Figure 8). Individually, the highest P_i for the Mono Lake excursion are obtained for Lake Pupuke, New Zealand (Nilsson et al., 2011) ($P_i = 2.2$ at 31.9 ka); ded8707, Mediterranean Sea (Tric et al., 1992) ($P_i = 1.1$ at 35.13 ka); ODP919, Irminger Basin (Channell, 2006) ($P_i = 0.9$ at 32.72 ka); ps2644-5, Iceland Basin (Laj et al., 2000) ($P_i = 0.8$ at 34.28 ka); ph05, Philippine Sea (Meng et al., 2009) ($P_i = 0.7$ at 34.11 ka); Summer Lake, Oregon (Negrini et al., 2014) ($P_i = 0.6$ at 34.17 ka); and 4-pc03, South Atlantic (Channell et al., 2000) ($P_i = 0.6$ at 34.34 ka). These P_i values are considerably lower than the P_i values for the Laschamp excursion (supporting information Table S3). The number of records that exhibit the Mono Lake excursion is smaller than for the Laschamp excursion records: when combined with the wide range of ages for the Mono Lake excursion, this contributes to a smooth signal over the time period. However, we do note that the Mono Lake is recorded in lavas from New Zealand (Cassata et al., 2008; Cassidy & Hill, 2009; Mochizuki et al., 2004, 2007) with ages in the range from 30 to 35 ka. Other excursions reported over the 0–100 ka period are Hilina Pali (~17 ka) (Coe et al., 1978; Singer et al., 2014), Norwegian-Greenland Sea excursion (~60 ka) (Laj & Channell, 2015; Nowaczyk et al., 1994), and Skálamælifell or post-Blake excursion (~100 ka) (Jicha et al., 2011; Singer, 2014). None are evident in the PSV index stacks, but appear in one record/location or have different timings, which lead to smoothing of

the averaged PSV index. The PSV indices averaged over the past 100 ka show only a small difference between the hemispheres, Northern versus Southern, and Atlantic versus Pacific hemisphere. However, the PSV activity index (σ_{P_i}) reveals that the Southern Hemisphere (σ_{P_i}=0.42) is more active than Northern (0.28), as well as the Atlantic (0.38) being more active than Pacific Hemisphere (0.11) over the past 100 ka. This suggests that the hemispheric asymmetry observed in the PSV activity index over the Holocene (Constable et al., 2016) may persist over longer timescales.

When geomagnetic excursions are well recorded, the PSV index allows us to estimate their durations (Figure 9). The duration is defined by the time span of the P_i index being higher than 0.5—the threshold value for transitional events. For example, the Laschamp excursion in m72/5–22 from Black Sea has a duration of 1,200 years characterized by transitional directions (VGPs between 45°N and 45°S) (Nowaczyk et al., 2012), but it lasts 1,300 years according to this approach (Figure 9). When we performed this analysis on all sediment records that demonstrate well defined peaks around the Laschamp excursion (supporting information Table S3), the average duration is again about 1,300 years, with values ranging from 350 to 3,100 years. For comparison, the average duration of the Laschamp excursion found by Leonhardt et al. (2009) in the IMOLEe model is 1,100 years with longer durations (~2,000 years) in the region of Mexico and the East Asia. Laj and Kissel (2015) estimated the duration of the Laschamp excursion considering separately directional changes and the intensity low: the first approach gave a duration of 640 years, while for the second, estimates vary between 1,500 and 3,000 years depending on whether only the GLOPIS-75 stack is used or it is combined with cosmogenic isotopes records.

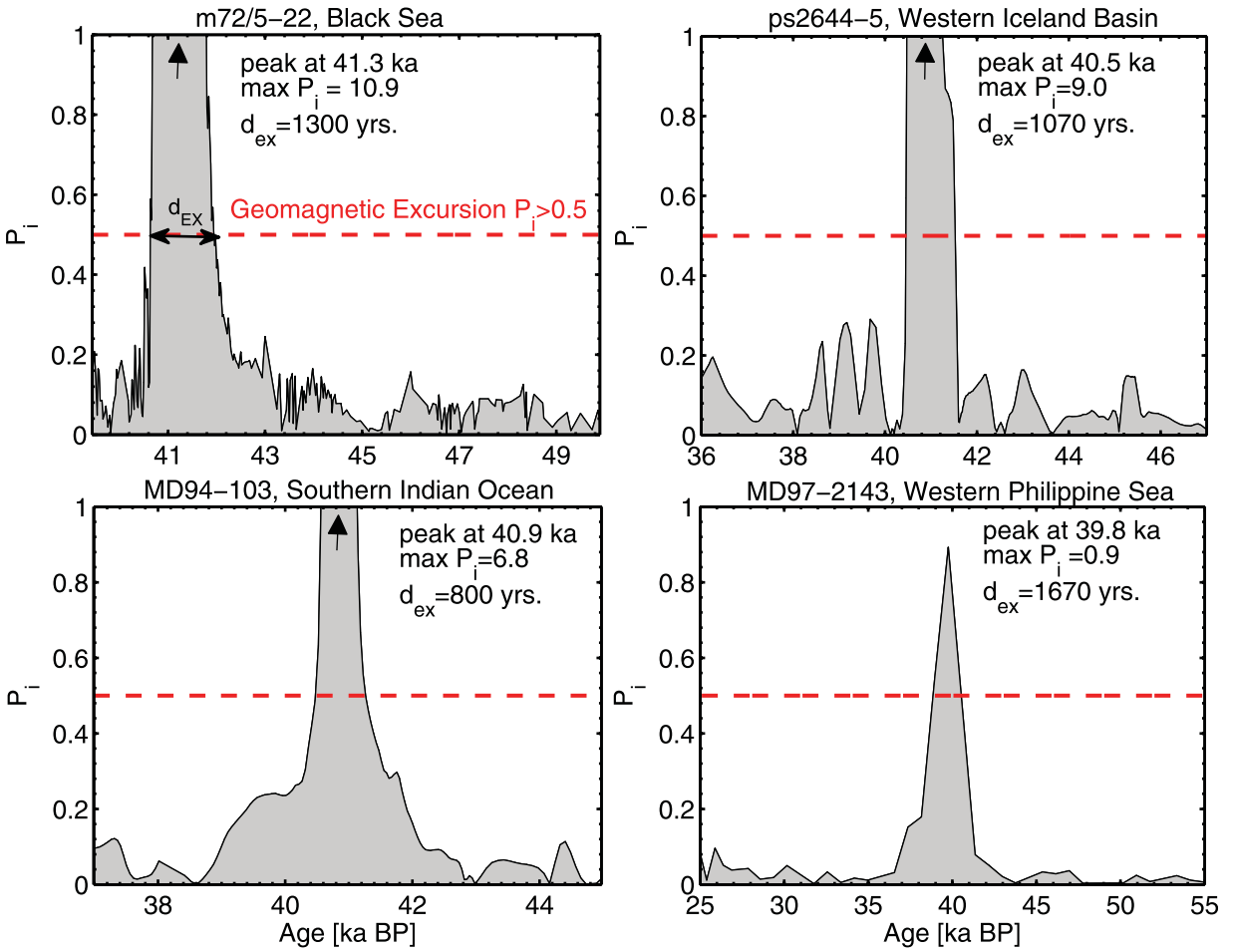

Figure 9. Estimates of the age and duration of the Laschamp excursion recorded in sediment paleomagnetic records using the PSV index. Four examples are presented: m72/5–22, Black Sea (Nowaczyk et al., 2012); ps2644-5, Western Iceland Basin (Laj et al., 2000); MD94–103, Southern Indian Ocean (Mazaud et al., 2002); and MD97–2143, Western Philippine Sea (Horng et al., 2003).

Supporting information Figures S7–S11 show the PSV index variations for the regional and global paleointensity stacks: GLOPIS-75, SAPIS, NAPIS-75, and NOPAPIS-250. In all stacks the maximum index corresponds to the Laschamp excursion. However, for the NOPAPIS-250 stack very low index values are obtained, below the threshold for transitional events, 0.5. Since the sediment records that form the NOPAPIS-250 stack have low sedimentation rates, it is quite probable that low resolution has contributed to smoothing of the PSV index values.

7. Conclusions

We have compiled directional and intensity data from archeological materials, volcanic rocks, and sediments covering the past 100 ka. Our compilation consists of 61,687 declination (116 records), 70,936 inclination (129 records), and 69,596 relative paleointensity data (157 records) from sediments and 4022 declination, 5704 inclination, and 5228 intensity archeomagnetic and volcanic data. Uncertainties for the sediment records have been estimated by smoothing spline models. Median uncertainties are: 5.8° for inclination (IQR: 3.2° to 8.2°), 15.2° for declination (IQR: 8.4° to 31.2°), and 0.4 for standardized RPI (IQR: 0.2 to 0.6). The temporal resolution of the records defined by the smoothing time ranges from 40 years to 13.8 ka (median: 400 years). Quantification of data uncertainty is important for building reliable paleomagnetic field models since they will ensure proper weighting and fit to the sediment magnetic records in the forthcoming 100 ka paleomagnetic field reconstructions.

The comparison of the paleomagnetic records with available field models and global/regional RPI stacks shows good agreement of the long-wavelength trends of geomagnetic field variations. Some differences can be attributed to chronological discrepancies among the data, stacks, and models. Although relative paleointensity stacks are invaluable for studying past geomagnetic field variations, the limited number of records used, exclusion of directional components, and lack of a global description of the geomagnetic field and its spatial and temporal variations at the Earth's surface and the core-mantle boundary (CMB), reflect the need for a global, time-dependent model over the past 100 ka. Such a model lies beyond the scope of the current work. However, it is currently under development and is the subject of a future paper. The results of the present work highlight the importance of taking proper account of both uncertainty estimates and smoothing times inferred from the sediment records during the new modeling.

We used the PSV index (Panovska & Constable, 2017) to investigate the occurrence of geomagnetic field excursions. The Laschamp excursion is found globally in individual sediment records with high index values and an average duration of 1,300 years. In our regional analysis, we find a more pronounced record of the Laschamp excursion in the Northern Hemisphere curve compared to the Southern Hemisphere, and in the Atlantic than in the Pacific Hemisphere bootstrap curve. Certainly, the stacking process averages out the PSV index and misaligned sediment records contribute to reducing the regional PSV index. The global, as well as the regional stacks show no anomalous/transitional activity at the time of the Mono Lake excursion. Likewise, other reported excursions during the past 100 ka are not clearly seen in the bootstrapped PSV index curves. The absence may be due to low sedimentation rates that filter out geomagnetic excursions, discrepancies in age scales, and large age errors in the individual paleomagnetic records, and/or the lack of global character of these features.

The new global data compilation of sediment paleomagnetic records, archeomagnetic, and volcanic data presented in this study is by far the largest available data set and will be used to model the global evolution of the geomagnetic field over the past 100 ka and to investigate the changes in the geomagnetic field morphology at the CMB during geomagnetic excursions. The significant increase in data compared to previous compilations provides the basis for an improved study of the geomagnetic field compared to current models and RPI stacks covering these timescales.

Acknowledgments
This work has been supported under NSF grants EAR 1246826 and EAR 1623786. S. Panovska gratefully acknowledges support from the Swiss National Science Foundation grant PBEZP2–142912. M.C. Brown is funded by Deutsche Forschungsgemeinschaft (DFG) (German Research Foundation in English) SPP PlanetMag 1488 project BR4697/1. We thank the Helmholtz Zentrum Potsdam—Deutsches GFZ for their hospitality during our collaboration on this work. The authors wish to thank Patrick Arneitz and one anonymous reviewer for the constructive comments and suggestions. We would like to express our sincere thanks to all authors who shared their data with us personally, or made them available through supporting information materials and collaborative databases. Their publications are referenced in the main article as well as in the supporting information, where they are related to specific paleomagnetic records.

References

Andersen, K. K., Svensson, A., Johnsen, S. J., Rasmussen, S. O., Bigler, M., Röthlisberger, R., et al. (2006). The Greenland ice core chronology 2005, 15–42 ka. Part 1: Constructing the time scale. *Quaternary Science Reviews*, *25*(23–24), 3246–3257.

Arneitz, P., Egli, R., & Leonhardt, R. (2017a). Unbiased analysis of geomagnetic data sets and comparison of historical data with paleomagnetic and archeomagnetic records. *Reviews of Geophysics*, *55*, 5–39. https://doi.org/10.1002/2016RG000527

Arneitz, P., Leonhardt, R., Schnepp, E., Heilig, B., Mayrhofer, F., Kovacs, P., et al. (2017b). The HISTMAG database: Combining historical, archaeomagnetic and volcanic data. *Geophysical Journal International*, *210*(3), 1347–1359.

Barton, C. E., & McElhinny, M. W. (1981). A 10000 years geomagnetic secular variation record from three Australian maars. *Geophysical Journal of the Royal Astronomical Society*, *67*(2), 465–485.
Benson, L., Liddicoat, J., Smoot, J., Sarna-Wojcicki, A., Negrini, R., & Lund, S. (2003). Age of the Mono Lake excursion and associated tephra. *Quaternary Science Reviews*, *22*(2–4), 135–140.
Biggin, A. J., & Paterson, G. A. (2014). A new set of qualitative reliability criteria to aid inferences on palaeomagnetic dipole moment variations through geological time. *Frontiers of Earth Science*, *2*, 24.
Biggin, A. J., Strik, G. H. M. A., & Langereis, C. G. (2009). The intensity of the geomagnetic field in the late-Archaean: New measurements and an analysis of the updated IAGA palaeointensity database. *Earth, Planets and Space*, *61*(1), 9–22.
Björck, S., & Wohlfarth, B. (2001). ^{14}C chronostratigraphic techniques in paleolimnology. In W. M. Last, & J. P. Smol (Eds.), *Tracking environmental change using lake sediments. Volume 1: Basin analysis, coring, and chronological techniques* (pp. 205–245). Dordrecht, The Netherlands: Kluwer.
Blanchet, C. L., Thouveny, N., & de Garidel-Thoron, T. (2006). Evidence for multiple paleomagnetic intensity lows between 30 and 50 ka BP from a western Equatorial Pacific sedimentary sequence. *Quaternary Science Reviews*, *25*(9–10), 1039–1052.
Bonhommet, N., & Zähringer, J. (1969). Paleomagnetism and potassium argon age determinations of the Laschamp geomagnetic polarity event. *Earth and Planetary Science Letters*, *6*(1), 43–46.
Boudreau, B. P. (1994). Is burial velocity a master parameter for bioturbation? *Geochimica et Cosmochimica Acta*, *58*(4), 1243–1249.
Bourne, M., Mac Niocaill, C., Thomas, A. L., Knudsen, M. F., & Henderson, G. M. (2012). Rapid directional changes associated with a 6.5 kyr-long Blake geomagnetic excursion at the Blake-Bahama Outer Ridge. *Earth and Planetary Science Letters*, *333–334*, 21–34.
Bourne, M. D., Mac Niocaill, C., Thomas, A. L., & Henderson, G. M. (2013). High-resolution record of the Laschamp geomagnetic excursion at the Blake-Bahama Outer Ridge. *Geophysical Journal International*, *195*, 1519–1533.
Brandt, U., Nowaczyk, N. R., Ramrath, A., Brauer, A., Mingram, J., Wulf, S., et al. (1999). Palaeomagnetism of Holocene and Late Pleistocene sediments from Lago di Mezzano and Lago Grande di Monticchio (Italy): Initial results. *Quaternary Science Reviews*, *18*(7), 961–976.
Brown, H. A. (1991). *A palaeomagnetic, geochronological and palaeoenvironmental investigation of Late and Post Glacial Maar Lake sediments from NW-Europe* (PhD thesis). Edinburgh, UK: University of Edinburgh.
Brown, M. C., Donadini, F., Korte, M., Nilsson, A., Korhonen, K., Lodge, A., et al. (2015a). GEOMAGIA50.v3: 1. General structure and modifications to the archeological and volcanic database. *Earth, Planets and Space*, *67*, 83.
Brown, M. C., Donadini, F., Nilsson, A., Panovska, S., Frank, U., Korhonen, K., et al. (2015b). GEOMAGIA50.v3: 2. A new paleomagnetic database for lake and marine sediments. *Earth, Planets and Space*, *67*(1), 70.
Brown, M. C., & Korte, M. (2016). A simple model for geomagnetic field excursions and inferences for palaeomagnetic observations. *Physics of the Earth and Planetary Interiors*, *254*, 1–11.
Cande, S. C., & Kent, D. V. (1995). Revised calibration of the geomagnetic polarity timescale for the Late Cretaceous and Cenozoic. *Journal of Geophysical Research*, *100*(B4), 6093–6095.
Carcaillet, J., Bourlès, D. L., Thouveny, N., & Arnold, M. (2004). A high resolution authigenic ^{10}Be/^{9}Be record of geomagnetic moment variations over the last 300 ka from sedimentary cores of the Portuguese margin. *Earth and Planetary Science Letters*, *219*(3–4), 397–412.
Cassata, W. S., Singer, B. S., & Cassidy, J. (2008). Laschamp and Mono Lake geomagnetic excursions recorded in New Zealand. *Earth and Planetary Science Letters*, *268*(1–2), 76–88.
Cassidy, J., & Hill, M. J. (2009). Absolute palaeointensity study of the Mono Lake excursion recorded by New Zealand basalts. *Physics of the Earth and Planetary Interiors*, *172*(3–4), 225–234.
Channell, J. E. T. (1999). Geomagnetic paleointensity and directional secular variation at Ocean Drilling Program (ODP) Site 984 (Bjorn Drift) since 500 ka: Comparisons with ODP Site 983 (Gardar Drift). *Journal of Geophysical Research*, *104*(B10), 22937–22951.
Channell, J. E. T. (2006). Late Brunhes polarity excursions (Mono Lake, Laschamp, Iceland Basin and Pringle Falls) recorded at ODP Site 919 (Irminger Basin). *Earth and Planetary Science Letters*, *244*(1–2), 378–393.
Channell, J. E. T., & Guyodo, Y. (2004). The Matuyama Chronozone at ODP Site 982 (Rockall Bank): Evidence for decimeter-scale magnetization lock-in depths. In J. E. T. Channell et al. (Eds.), *Timescales of the paleomagnetic field, Geophysical monograph series* (Vol. 145, pp. 205–219). Washington, DC: American Geophysical Union.
Channell, J. E. T., Hodell, D. A., & Curtis, J. H. (2012b). ODP Site 1063 (Bermuda Rise) revisited: Oxygen isotopes, excursions and paleointensity in the Brunhes Chron. *Geochemistry, Geophysics, Geosystems*, *13*, Q02001. https://doi.org/10.1029/2011GC003897
Channell, J. E. T., Hodell, D. A., & Lehman, B. (1997). Relative geomagnetic paleointensity and δ^{18}O at ODP Site 983 (Gardar Drift, North Atlantic) since 350 ka. *Earth and Planetary Science Letters*, *153*(1–2), 103–118.
Channell, J. E. T., Hodell, D. A., Romero, O., Hillaire-Marcel, C., de Vernal, A., Stoner, J. S., et al. (2012a). A 750-kyr detrital-layer stratigraphy for the North Atlantic (IDOP Sites U1302-U1303, Orphan Knoll, Labrador Sea). *Earth and Planetary Science Letters*, *317–318*, 218–230.
Channell, J. E. T., Hodell, D. A., Xuan, C., Mazaud, A., & Stoner, J. S. (2008). Age calibrated relative paleointensity for the last 1.5 Myr at IODP Site U1308 (North Atlantic). *Earth and Planetary Science Letters*, *274*(1–2), 59–71.
Channell, J. E. T., & Raymo, M. E. (2003). Paleomagnetic record at ODP Site 980 (Feni Drift, Rockall) for the past 1.2 Myrs. *Geochemistry, Geophysics, Geosystems*, *4*(4), 1033. https://doi.org/10.1029/2002GC000440
Channell, J. E. T., Stoner, J. S., Hodell, D., & Charles, C. D. (2000). Geomagnetic paleointensity for the last 100 kyr from the sub-Antarctic South Atlantic: A tool for inter-hemispheric correlation. *Earth and Planetary Science Letters*, *175*(1–2), 145–160.
Channell, J. E. T., Xuan, C., & Hodell, D. A. (2009). Stacking paleointensity and oxygen isotope data for the last 1.5 Myr (PISO-1500). *Earth and Planetary Science Letters*, *283*(1–4), 14–23.
Coe, R. S., Grommé, S., & Mankinen, E. (1978). Geomagnetic paleointensities from radiocarbon-dated lava flows on Hawaii and the question of the Pacific Nondipole Low. *Journal of Geophysical Research*, *83*(B4), 1740–1756.
Collins, L. G., Hounslow, M. W., Allen, C. S., Hodgson, D. A., Pike, J., & Karloukovski, V. V. (2012). Palaeomagnetic and biostratigraphic dating of marine sediments from the Scotia Sea, Antarctica: First identification of the Laschamp excursion in the Southern Ocean. *Quaternary Geochronology*, *7*, 67–75.
Constable, C. G. (1985). Eastern Australian geomagnetic field intensity over the past 14000 yr. *Geophysical Journal of the Royal Astronomical Society*, *81*(1), 121–130.
Constable, C. G., Korte, M., & Panovska, S. (2016). Persistent high paleosecular variation activity in southern hemisphere for at least 10 000 years. *Earth and Planetary Science Letters*, *453*, 78–86.
Constable, C. G., & Parker, R. L. (1991). Deconvolution of long-core palaeomagnetic measurements - spline therapy for the linear problem. *Geophysical Journal International*, *104*(3), 453–468.
Constable, C. G., & Tauxe, L. (1987). Palaeointensity in the pelagic realm: Marine sediment data compared with archaeomagnetic and lake sediment records. *Geophysical Journal of the Royal Astronomical Society*, *90*(1), 43–59.

Creer, K. M., Hogg, T. E., Readman, P. W., & Reynaud, C. (1980). Palaeomagnetic secular variation curves extending back to 13,400 years B.P. recorded by sediments deposited in Lac de Joux, Switzerland. *Journal of Geophysics*, *48*, 139–147.
Creer, K. M., Valencio, D. A., Sinito, A. M., Tucholka, P., & Vilas, J. F. A. (1983). Geomagnetic secular variations 0–14 000 yr BP as recorded by lake sediments from Argentina. *Geophysical Journal of the Royal Astronomical Society*, *74*(1), 199–221.
Cromwell, G., Johnson, C. L., Tauxe, L., Constable, C. G., & Jarboe, N. (2018). PSV10: A global data set for 0–10 Ma time-averaged field and paleosecular variation studies. *Geochemistry, Geophysics, Geosystems*. https://doi.org/10.1002/2017GC007318
Dodson, R., Fuller, M., & Pilant, W. (1974). On the measurement of the remanent magnetism of long cores. *Geophysical Research Letters*, *1*(4), 185–188.
Dansgaard, W., Johnsen, S. J., Clausen, H. B., Dahl-Jensen, D., Gundestrup, N. S., Hammer, C. U., et al. (1993). Evidence for general instability of past climate from a 250-kyr ice-core record. *Nature*, *364*(6434), 218–220.
De Boor, C. (2001). *A practical guide to splines*. New York, NY: Springer.
Demory, F., Nowaczyk, N. R., Witt, A., & Oberhänsli, H. (2005). High resolution magnetostratigraphy of late Quaternary sediments from Lake Baikal, Siberia: Timing of intracontinental paleoclimatic responses. *Global and Planetary Change*, *46*(1–4), 167–186.
Denham, C. R., & Cox, A. (1971). Evidence that the Laschamp polarity event did not occur 13,300-34,000 years ago. *Earth and Planetary Science Letters*, *13*(1), 181–190.
Diepenbroek, M., Grobe, H., Reinke, M., Schindler, U., Schlitzer, R., Sieger, R., et al. (2002). PANGAEA: An information system for environmental sciences. *Computers & Geosciences*, *28*(10), 1201–1210.
Donadini, F., Korte, M., & Constable, C. G. (2009). Geomagnetic field for 0–3 ka: 1. New data sets for global modelling. *Geochemistry, Geophysics, Geosystems*, *10*, Q06007. https;//doi.org/10.1029/2008GC002295
Egli, R., & Zhao, X. (2015). Natural remanent magnetization acquisition in bioturbated sediment: General theory and implications for relative paleointensity reconstructions. *Geochemistry, Geophysics, Geosystems*, *16*, 995–1016. https://doi.org/10.1002/2014GC005672
Expedition 303 Scientists. (2006). Site U1305. In J. E. T. Channell et al. (Eds.), *Proceedings of the international ocean discovery program* (Vol. 303/306). College Station, TX: International Ocean Discovery Program.
Fisher, R. A. (1953). Dispersion on a sphere. *Proceedings of the Royal Society of London. Series A*, *217*(1130), 295–305.
Frank, U. (2007). Palaeomagnetic investigations on lake sediments from NE China: A new record of geomagnetic secular variations for the last 37 ka. *Geophysical Journal International*, *169*(1), 29–40.
Frank, U., Nowaczyk, N. R., Negendank, J. F. W., & Melles, M. (2002). A paleomagnetic record from Lake Lama, northern Central Siberia. *Physics of the Earth and Planetary Interiors*, *133*(1–4), 3–20.
Ge, S.-L., Løvlie, R., Shi, X.-F., Fang, X.-S., Chen, Z.-H., & Wu, Y.-H. (2013). Relative paleointensity recorded in the core from Northwestern Philippine Sea over the last 125 ka and its influencing factors. *Chinese Journal of Geophysics*, *56*(1), 27–42.
Geiss, C. E., & Banerjee, S. K. (2003). A Holocene-Late Pleistocene geomagnetic inclination record from Grandfather Lake, SW Alaska. *Geophysical Journal International*, *153*(2), 497–507.
Geiss, C. E., Dorale, J. A., & Dahms, D. (2007). A rockmagnetic and palaeomagnetic record of two glacial lakes in the Wind River Range, Wyoming, USA. *EOS Transactions of American Geophysical Union*, *88*(52), Abstract GP53B-1216.
Gogorza, C. S. G., Irurzun, M. A., Chaparro, M. A. E., Lirio, J. M., Nuñez, H., Bercoff, P. G., et al. (2006). Relative paleointensity of the geomagnetic field over the last 21,000 years BP from sediment cores, Lake El Trébol (Patagonia, Argentina). *Earth, Planets and Space*, *58*(10), 1323–1332.
Gogorza, C. S. G., Irurzun, M. A., Sinito, A. M., Lisé-Pronovost, A., St-Onge, G., Haberzettl, T., et al. (2012). High-resolution paleomagnetic records from Laguna Potrok Aike (Patagonia, Argentina) for the last 16,000 years. *Geochemistry, Geophysics, Geosystems*, *13*, Q12Z37. https://doi.org/10.1029/2011GC003900
Gogorza, C. S. G., Lirio, J. M., Nuñez, H., Chaparro, M., Bertorello, H. R., & Sinito, A. M. (2004). Paleointensity studies on Holocene-Pleistocene sediments from Lake Escondido, Argentina. *Physics of the Earth and Planetary Interiors*, *145*(1–4), 219–238.
Green, P. J., & Silverman, B. W. (1994). *Nonparametric regression and generalized linear models: A roughness penalty approach*. London, UK: CRC Press.
Griffiths, D. H. (1955). The remanent magnetism of varved clays from Sweden. *Monthly Notices of the Royal Astronomical Society Supplement*, *7*, 103–114.
GRIP members. (1993). Climate instability during the last interglacial period recorded in the GRIP ice core. *Nature*, *364*, 203–207.
Grootes, P. M., & Stuiver, M. (1997). Oxygen 18/16 variability in Greenland snow and ice with $10^{-3}-$ to $10^{5}-$year time resolution. *Journal of Geophysical Research*, *102*(C12), 26455–26470.
Guyodo, Y., Channell, J. E. T., & Thomas, R. G. (2002). Deconvolution of u-channel paleomagnetic data near geomagnetic reversals and short events. *Geophysical Research Letters*, *29*(17), 1845. https://doi.org/10.1029/2002GL014927
Guyodo, Y., Richter, C., & Valet, J. P. (1999). Paleointensity record from Pleistocene sediments (1.4-0 Ma) off the California Margin. *Journal of Geophysical Research*, *104*(B10), 22953–22965.
Guyodo, Y., & Valet, J.-P. (1996). Relative variations in geomagnetic intensity from sedimentary records: The past 200,000 years. *Earth and Planetary Science Letters*, *143*(1–4), 23–36.
Guyodo, Y., & Valet, J.-P. (1999). Global changes in intensity of the Earth's magnetic field during the past 800 kyr. *Nature*, *399*(6733), 249–252.
Haag, M. (2000). Reliability of relative palaeointensity of a sediment core with climatically-triggered strong magnetization changes. *Earth and Planetary Science Letters*, *180*(1–2), 49–59.
Haberzettl, T., Henkel, K., Kasper, T., Ahlborn, M., Su, Y., Wang, J., et al. (2015). Independently dated paleomagnetic secular variation records from the Tibetan Plateau. *Earth and Planetary Science Letters*, *416*, 98–108.
Hayashida, A., Ali, M., Kuniko, Y., Kitagawa, H., Torii, M., & Takemura, K. (2007). Environmental magnetic record and paleosecular variation data for the last 40 kyrs from the Lake Biwa sediments, Central Japan. *Earth, Planets and Space*, *59*(7), 807–814.
Hayashida, A., Verosub, K. L., Heider, F., & Leonhardt, R. (1999). Magnetostratigraphy and relative palaeointensity of late Neogene sediments at ODP Leg 167 Site 1010 off Baja California. *Geophysical Journal International*, *139*(3), 829–840.
Henkel, K., Haberzettl, T., St-Onge, G., Wang, J., Ahlborn, M., Daut, G., et al. (2016). High-resolution paleomagnetic and sedimentological investigations on the Tibetan Plateau for the past 16 ka cal B.P.: The Tangra Yumco record. *Geochemistry, Geophysics, Geosystems*, *17*, 774–790. https://doi.org/10.1002/2015GC006023
Hillenbrand, C.-D., Smith, J. A., Kuhn, G., Esper, O., Gersonde, R., Larter, R. D., et al. (2010). Age assignment of a diatomaceous ooze deposited in the western Amundsen Sea Embayment after the Last Glacial Maximum. *Journal of Quaternary Science*, *25*(3), 280–295.
Horng, C. S., Roberts, A. P., & Liang, W. T. (2003). A 2.14-Myr astronomically tuned record of relative geomagnetic paleointensity from the western Philippine Sea. *Journal of Geophysical Research*, *108*(B1), 2059.

Hua, Q., Barbetti, M., Fink, D., Kaiser, K. F., Friedrich, M., Kromer, B., et al. (2009). Atmospheric ^{14}C variations derived from tree rings during the early Younger Dryas. *Quaternary Science Reviews*, *28*(25–26), 2982–2990.
Huang, Y.-S., Lee, T.-Q., Hsu, S.-K., & Yang, T.-N. (2009). Paleomagnetic field variation with strong negative inclination during the Brunhes chron at the Banda Sea, equatorial southwestern Pacific. *Physics of the Earth and Planetary Interiors*, *173*(1–2), 162–170.
Hyodo, M. (1984). Possibility of reconstruction of the past geomagnetic field from homogeneous sediments. *Journal of Geomagnetism and Geoelectricity*, *36*(2), 45–62.
Hyodo, M., Itota, C., & Yaskawa, K. (1993). Geomagnetic secular variation reconstructed from magnetizations of wide-diameter cores of Holocene sediments in Japan. *Journal of Geomagnetism and Geoelectricity*, *45*(8), 669–969.
Imbrie, J., Hays, J. D., Martinson, D. G., McIntyre, A., Mix, A. C., Morley, J. J., et al. (1984). The orbital theory of Pleistocene climate: Support from a revised chronology of the marine $\delta^{18}O$ record. In A. L. Berger et al. (Eds.), *Milankovitch and climate, Part I*. (Vol. 126, pp. 269–305). Kufstein, Austria: Reidel.
Ingham, E., Turner, G. M., Conway, C. E., Heslop, D., Roberts, A. P., Leonard, G., et al. (2017). Volcanic records of the Laschamp geomagnetic excursion from Mt Ruapehu, New Zealand. *Earth and Planetary Science Letters*, *472*, 131–141.
Irurzun, M. A., Gogorza, C. S. G., Torcida, S., Lirio, J. M., Nuñez, H., Bercoff, P. G., et al. (2009). Rock magnetic properties and relative paleointensity stack between 13 and 24 kyr BP calibrated ages from sediment cores, Lake Moreno (Patagonia, Argentina). *Physics of the Earth and Planetary Interiors*, *172*(3–4), 157–168.
Irving, E., & Major, A. (1964). Post-depositional detrital remanent magnetization in a synthetic sediment. *Sedimentology*, *3*(2), 135–143.
Jackson, A., Jonkers, A. R. T., & Walker, M. R. (2000). Four centuries of geomagnetic secular variation from historical records. *Philosophical Transactions of the Royal Society of London A*, *358*(1768), 957–990.
Jackson, M., Bowles, J. A., Lascu, I., & Solheid, P. (2010). Deconvolution of u channel magnetometer data: Experimental study of accuracy, resolution, and stability of different inversion methods. *Geochemistry, Geophysics, Geosystems*, *11*, Q07Y10. https://doi.org/10.1029/2009GC002991
Jicha, B. R., Kristjánsson, L., Brown, M. C., Singer, B. S., Beard, B. L., & Johnson, C. M. (2011). New age for the Skálamælifell excursion and identification of a global geomagnetic event in the late Brunhes chron. *Earth and Planetary Science Letters*, *310*(3–4), 509–517.
Johnson, C. L., & Constable, C. G. (1995). The time-averaged geomagnetic field as recorded by lava flows over the past 5 Myr. *Geophysical Journal International*, *122*(2), 489–519.
Johnson, C. L., & Constable, C. G. (1997). The time-averaged geomagnetic field: Global and regional biases for 0–5 Ma. *Geophysical Journal International*, *131*(3), 643–666.
Johnson, E. A., Murphy, T., & Torreson, O. W. (1948). Pre-history of the Earth's magnetic field. *Journal of Geophysical Research*, *53*(4), 349–372.
Karlin, R. (1984). *Paleomagnetism, rock magnetism and diagenesis in hemipelagic sediments from the northeast Pacific Ocean and the Gulf of California* (PhD thesis). Corvallis, OR: Oregon State University.
Kelly, P., & Gubbins, D. (1997). The geomagnetic field over the past 5 million years. *Geophysical Journal International*, *128*(2), 315–330.
Kent, D. V., & Opdyke, N. D. (1977). Paleomagnetic field intensity variation recorded in a Brunhes epoch deep-sea sediment core. *Nature*, *266*(5598), 156–159.
King, R. F. (1955). The remanent magnetism of artificially deposited sediments. *Monthly Notices of the Royal Astronomical Society*, *7*, 115–134.
Kirschvink, J. L. (1980). The least-squares line and plane and the analysis of palaeomagnetic data. *Geophysical Journal of the Royal Astronomical Society*, *62*(3), 699–718.
Kissel, C., Guillou, H., Laj, C., Carracedo, J. C., Nomade, S., Perez-Torrado, F., et al. (2011). The Mono Lake excursion recorded in phonolitic lavas from Tenerife (Canary Islands): Paleomagnetic analyses and coupled K/Ar and Ar/Ar dating. *Physics of the Earth and Planetary Interiors*, *187*(3–4), 232–244.
Kissel, C., Laj, C., Labeyrie, L., Dokken, T., Voelker, A., & Blamart, D. (1999). Rapid climatic variations during marine isotopic stage 3: Magnetic analysis of sediments from Nordic Seas and North Atlantic. *Earth and Planetary Science Letters*, *171*(3), 489–502.
Kliem, P., Enters, D., Hahn, A., Ohlendorf, C., Lisé-Pronovost, A., St-Onge, G., et al. (2013). Lithology, radiocarbon dating and sedimentological interpretation of the 51 ka BP lacustrine record from Laguna Potrok Aike, southern Patagonia. *Quaternary Science Reviews*, *71*, 54–69.
Knudsen, M. F., Riisager, P., Donadini, F., Snowball, I., Muscheler, R., Korhonen, K., et al. (2008). Variations in the geomagnetic dipole moment during the Holocene and the past 50 kyr. *Earth and Planetary Science Letters*, *272*(1–2), 319–329.
Korhonen, K., Donadini, F., Riisager, P., & Pesonen, L. J. (2008). Geomagia50: An archeointensity database with PHP and MySQL. *Geochemistry, Geophysics, Geosystems*, *9*, Q04029. https://doi.org/10.1029/2007GC001893
Korte, M., & Constable, C. G. (2003). Continuous global geomagnetic field models for the past 3000 years. *Physics of the Earth and Planetary Interiors*, *140*(1–3), 73–89.
Korte, M., & Constable, C. G. (2005). Continuous geomagnetic field models for the past 7 millennia: 2. CALS7K. *Geochemistry, Geophysics, Geosystems*, *6*, Q02H16. https://doi.org/10.1029/2004GC000801
Korte, M., & Constable, C. G. (2006). On the use of calibrated relative paleointensity records to improve millennial: Scale geomagnetic field models. *Geochemistry, Geophysics, Geosystems*, *7*, Q09004. https://doi.org/10.1029/2006GC001368
Korte, M., & Constable, C. G. (2011). Improving geomagnetic field reconstructions for 0–3 ka. *Physics of the Earth and Planetary Interiors*, *188*(3–4), 247–259.
Korte, M., Constable, C. G., Donadini, F., & Holme, R. (2011). Reconstructing the Holocene geomagnetic field. *Earth and Planetary Science Letters*, *312*(3–4), 497–505.
Korte, M., Donadini, F., & Constable, C. G. (2009). Geomagnetic field for 0–3 ka: 2. A new series of time-varying global models. *Geochemistry, Geophysics, Geosystems*, *10*, Q06008. https://doi.org/10.1029/2008GC002297
Korte, M., Genevey, A., Constable, C. G., Frank, U., & Schnepp, E. (2005). Continuous geomagnetic field models for the past 7 millennia: 1. A new global data compilation. *Geochemistry, Geophysics, Geosystems*, *6*, Q02H15. https://doi.org/10.1029/2004GC000800
Kristjansson, L., & Gudmundsson, A. (1980). Geomagnetic excursion in late-glacial basalt outcrops in South-Western Iceland. *Geophysical Research Letters*, *7*(5), 337–340.
Laj, C., & Channell, J. E. T. (2015). Chapter 5.10: Geomagnetic excursions. In G. Schubert (Ed.), *Treatise on geophysics* (pp. 343–383). New York, NY: Elsevier.
Laj, C., & Kissel, C. (2015). An impending geomagnetic transition? Hints from the past. *Frontiers of Earth Science*, *3*, 61.
Laj, C., Kissel, C., & Beer, J. (2004). High resolution global paleointensity stack since 75 kyr (GLOPIS-75) calibrated to absolute values. In J. E. T. Channell et al. (Eds.), *Timescales of the paleomagnetic field, Geophysical monograph series* (Vol. 145, pp. 255–265). Washington, DC: American Geophysical Union.

Laj, C., Kissel, C., Mazaud, A., Channell, J. E. T., & Beer, J. (2000). North Atlantic paleointensity stack since 75 ka (NAPIS-75) and the duration of the Laschamp event. *Philosophical Transactions of the Royal Society of London A*, *358*(1768), 1009–1025.
Laj, C., Kissel, C., & Roberts, A. P. (2006). Geomagnetic field behavior during the Iceland Basin and Laschamp geomagnetic excursions: A simple transitional field geometry? *Geochemistry, Geophysics, Geosystems*, *7*, Q03004. https://doi.org/10.1029/2005GC001122
Lascu, I., Feinberg, J. M., Dorale, J. A., Cheng, H., & Edwards, R. L. (2016). Age of the Laschamp excursion determined by U-Th dating of a speleothem geomagnetic record from North America. *Geology*, *44*(2), 139–142.
Lebreiro, S. M., Voelker, A. H. L., Vizcaino, A., Abrantes, F. G., Alt-Epping, U., Jung, S., et al. (2009). Sediment instability on the Portuguese continental margin under abrupt glacial climate changes (last 60 kyr). *Quaternary Science Reviews*, *28*(27–28), 3211–3223.
Lehman, B., Laj, C., Kissel, C., Mazaud, A., Paterne, M., & Labeyrie, L. (1996). Relative changes of the geomagnetic field intensity during the last 280 kyr from piston cores in the Açores area. *Physics of the Earth and Planetary Interiors*, *93*(3–4), 269–284.
Leonhardt, R., Fabian, K., Winklhofer, M., Ferk, A., Laj, C., & Kissel, C. (2009). Geomagnetic field evolution during the Laschamp excursion. *Earth and Planetary Science Letters*, *278*(1–2), 87–95.
Levi, S., Audunsson, H., Duncan, R. A., Kristjansson, L., Gillot, P.-Y., & Jakobsson, S. P. (1990). Late Pleistocene geomagnetic excursion in Icelandic lavas: Confirmation of the Laschamp excursion. *Earth and Planetary Science Letters*, *96*(3–4), 443–457.
Levi, S., & Karlin, R. (1989). A sixty thousand year paleomagnetic record from Gulf of California sediments: Secular variation, late Quaternary excursions and geomagnetic implications. *Earth and Planetary Science Letters*, *92*(2), 219–233.
Licht, A., Hulot, G., Gallet, Y., & Thébault, E. (2013). Ensembles of low degree archeomagnetic field models for the past three millennia. *Physics of the Earth and Planetary Interiors*, *224*, 38–67.
Lisé-Pronovost, A., St-Onge, G., Gogorza, C. S. G., Haberzettl, T., Preda, M., Kliem, P., et al. (2013). High-resolution paleomagnetic secular variations and relative paleointensity since the Late Pleistocene in southern South America. *Quaternary Science Reviews*, *71*, 91–108.
Lisiecki, L. E., & Raymo, M. E. (2005). A Pliocene-Pleistocene stack of 57 globally distributed benthic $\delta^{18}O$ records. *Paleoceanography*, *20*, PA1003. https://doi.org/10.1029/2004PA001071
Lund, S. P., & Keigwin, L. (1994). Measurement of the degree of smoothing in sediment paleomagnetic secular variation records: An example from Late Quaternary deep - sea sediments of the Bermuda Rise, western North Atlantic ocean. *Earth and Planetary Science Letters*, *122*(3–4), 317–330.
Lund, S. P., Schwartz, M., Keigwin, L., & Johnson, T. (2005). Deep-sea sediment records of the Laschamp geomagnetic field excursion (~41,000 calendar years before present). *Journal of Geophysical Research*, *110*, B04101. https://doi.org/10.1029/2003JB002943
Lund, S. P., Stoner, J., & Lamy, F. (2006a). 2. Late Quaternary paleomagnetic secular variation and chronostratigraphy from ODP Sites 1233 and 1234. In R. Tiedemann et al. (Eds.), *Proceedings of ocean drilling program, science results* (Vol. 202, pp 1–22). College Station, TX: International Ocean Discovery Program.
Lund, S. P., Stott, L., Schwartz, M., Thunell, R., & Chen, A. (2006). Holocene paleomagnetic secular variation records from the western Equatorial Pacific Ocean. *Earth and Planetary Science Letters*, *246*(3–4), 381–392.
Macrì, P., Sagnotti, L., Dinarès-Turell, J., & Caburlotto, A. (2005). A composite record of Late Pleistocene relative geomagnetic paleointensity from the Wilkes Land Basin (Antarctica). *Physics of the Earth and Planetary Interiors*, *151*(3–4), 223–242.
Marco, S., Ron, H., McWilliams, M. O., & Stein, M. (1998). High-resolution record of geomagnetic secular variation from Late Pleistocene Lake Lisan sediments (paleo Dead Sea). *Earth and Planetary Science Letters*, *161*(1–4), 145–160.
Martinson, D. G., Pisias, N. G., Hays, J. D., Imbrie, J., Moore, T. C., Jr., & Shackleton, N. J. (1987). Age dating and the orbital theory of the Ice Ages: Development of a high-resolution 0 to 300,000-year chronostratigraphy. *Quaternary Research*, *27*(01), 1–29.
Mazaud, A., Channell, J. E. T., & Stoner, J. S. (2012). Relative paleointensity and environmental magnetism since 1.2 Ma at IODP site U1305 (Eirik Drift, NW Atlantic). *Earth and Planetary Science Letters*, *357–358*, 137–144.
Mazaud, A., Channell, J. E. T., & Stoner, J. S. (2015). The paleomagnetic record at IODP Site U1307 back to 2.2 Ma (Eirik Drift, off south Greenland). *Earth and Planetary Science Letters*, *429*, 82–89.
Mazaud, A., Sicre, M. A., Ezat, U., Pichon, J. J., Duprat, J., Laj, C., et al. (2002). Geomagnetic-assisted stratigraphy and sea surface temperature changes in core MD94–103 (Southern Indian Ocean): Possible implications for North-South climatic relationships around H4. *Earth and Planetary Science Letters*, *201*(1), 159–170.
Meese, D. A., Gow, A. J., Alley, R. B., Zielinski, G. A., Grootes, P. M., Ram, M., et al. (1997). The Greenland Ice Sheet Project 2 depth-age scale: Methods and results. *Journal of Geophysical Research*, *102*(C12), 26367–26423.
Meng, Q. Y., Li, A. C., Li, T. G., Jiang, F. Q., & Zhou, X. J. (2009). Relative paleointensity of the geomagnetic field during the past 200 ka from the West Philippine Sea and its chronological significance. *Science in China Series D*, *52*(8), 1115–1126.
Meynadier, L., Valet, J. P., & Shackleton, N. J. (1995). Chapter: 38. Relative geomagnetic intensity during the last 4 m.y. from the Equatorial Pacific. In N. Pisias et al. (Eds.), *Proceedings of the ocean drilling program, science results* (Vol. 138, pp. 779–795). College Station, TX: International Ocean Discovery Program.
Meynadier, L., Valet, J. P., Weeks, R., Shackleton, N. J., & Hagee, V. L. (1992). Relative geomagnetic intensity of the field during the last 140 ka. *Earth and Planetary Science Letters*, *114*(1), 39–57.
Mochizuki, N., Tsunakawa, H., Shibuya, H., Tagami, T., Ozawa, A., Cassidy, J., et al. (2004). K-Ar ages of the Auckland geomagnetic excursions. *Earth, Planets and Space*, *56*(2), 283–288.
Mochizuki, N., Tsunakawa, H., Shibuya, H., Tagami, T., Ozawa, A., & Smith, I. E. M. (2007). Further K-Ar dating and paleomagnetic study of the Auckland geomagnetic excursions. *Earth, Planets and Space*, *59*(7), 755–761.
Mothersill, J. S. (1979). The paleomagnetic record of the late Quaternary sediments of Thunder Bay. *Canadian Journal of Earth Sciences*, *16*(5), 1016–1023.
Mothersill, J. S. (1981). Late Quaternary record of the Goderich Basin, Lake Huron. *Canadian Journal of Earth Sciences*, *18*(3), 448–456.
Muscheler, R., Adolphi, F., & Svensson, A. (2014). Challenges in ^{14}C dating towards the limit of the method inferred from anchoring a floating tree ring radiocarbon chronology to ice core records around the Laschamp geomagnetic field minimum. *Earth and Planetary Science Letters*, *394*, 209–215.
Negrini, R. M., McCuan, D. T., Horton, R. A., Lopez, J. D., Cassata, W. S., Channell, J. E. T., et al. (2014). Nongeocentric axial dipole field behavior during the Mono Lake excursion. *Journal of Geophysical Research: Solid Earth*, *119*, 2567–2581. https://doi.org/10.1002/2013JB010846
Nilsson, A., Holme, R., Korte, M., Suttie, N., & Hill, M. (2014). Reconstructing Holocene geomagnetic field variation: New methods, models and implications. *Geophysical Journal International*, *198*(1), 229–248.
Nilsson, A., Muscheler, R., Snowball, I., Aldahan, A., Possnert, G., Augustinus, P., et al. (2011). Multi-proxy identification of the Laschamp geomagnetic field excursion in Lake Pupuke, New Zealand. *Earth and Planetary Science Letters*, *311*(1–2), 155–164.
Nowaczyk, N. R. (1997). High-resolution magnetostratigraphy of four sediment cores from the Greenland Sea: II. Rock magnetic and relative palaeointensity data. *Geophysical Journal International*, *131*(2), 325–334.

Nowaczyk, N. R., & Antonow, M. (1997). High-resolution magnetostratigraphy of four sediment cores from the Greenland Sea: I. Identification of the Mono Lake excursion, Laschamp and Biwa I/Jamaica geomagnetic polarity events. *Geophysical Journal International*, *131*(2), 310–324.

Nowaczyk, N. R., Antonow, M., Knies, J., & Spielhagen, R. F. (2003). Further rock magnetic and chronostratigraphic results on reversal excursions during the last 50 ka as derived from northern high latitudes and discrepancies in precise AMS ^{14}C dating. *Geophysical Journal International*, *155*(3), 1065–1080.

Nowaczyk, N. R., Arz, H. W., Frank, U., Kind, J., & Plessen, B. (2012). Dynamics of the Laschamp geomagnetic excursion from Black Sea sediments. *Earth and Planetary Science Letters*, *351–352*, 54–69.

Nowaczyk, N. R., Frank, U., Kind, J., & Arz, H. W. (2013). A high-resolution paleointensity stack of the past 14 to 68 ka from Black Sea sediments. *Earth and Planetary Science Letters*, *384*, 1–16.

Nowaczyk, N. R., & Frederichs, T. W. (1999). Geomagnetic events and relative palaeointensity variations during the past 300 ka as recorded in Kolbeinsey Ridge sediments, Iceland Sea: Indication for a strongly variable geomagnetic field. *International Journal of Earth Sciences*, *88*(1), 116–131.

Nowaczyk, N. R., Frederichs, T. W., Eisenhauer, A., & Gard, G. (1994). Magnetostratigraphic data from late Quaternary sediments from the Yermak Plateau, Arctic Ocean: Evidence for four geomagnetic polarity events within the last 170 Ka of the Brunhes Chron. *Geophysical Journal International*, *117*(2), 453–471.

Nowaczyk, N. R., Frederichs, T. W., Kassens, H., Nørgaard-Pedersen, N., Spielhagen, R. F., Stein, R., et al. (2001). Sedimentation rates in the Makarov Basin, central Arctic Ocean: A paleomagnetic and rock magnetic approach. *Paleoceanography*, *16*(4), 368–389.

Nowaczyk, N. R., & Knies, J. (2000). Magnetostratigraphic results from the eastern Arctic Ocean: AMS ^{14}C ages and relative palaeointenisity data of the Mono Lake and Laschamp geomagnetic reversal excursions. *Geophysical Journal International*, *140*(1), 185–197.

Obrochta, S. P., Yokoyama, Y., Morén, J., & Crowley, T. J. (2014). Conversion of GISP2-based sediment core age models to the GICC05 extended chronology. *Quaternary Geochronology*, *20*, 1–7.

Oda, H., Nakamura, K., Ikehara, K., Nakano, T., Nishimura, M., & Khlystov, O. (2002). Paleomagnetic record from Academician Ridge, Lake Baikal: A reversal excursion at the base of marine oxygen isotope stage 6. *Earth and Planetary Science Letters*, *202*(1), 117–132.

Oda, H., & Shibuya, H. (1996). Deconvolution of long-core paleomagnetic data of Ocean Drilling Program by Akaike's Bayesian Information Criterion minimization. *Journal of Geophysical Research*, *101*(B2), 2815–2834.

Oda, H., Xuan, C., & Yamamoto, Y. (2016). Toward robust deconvolution of pass-through paleomagnetic measurements: New tool to estimate magnetometer sensor response and laser interferometry of sample positioning accuracy. *Earth, Planets and Space*, *68*(1), 1–13.

Ohno, M., Hamano, Y., Murayama, M., Matsumoto, E., Iwakura, H., Nakamura, T., et al. (1993). Paleomagnetic record over the past 35,000 years of a sediment core from off Shikoku, southwest Japan. *Geophysical Research Letters*, *20*(13), 1395–1398.

Ohno, M., Hamano, Y., Okamura, M., & Shimazaki, K. (1991). Geomagnetic secular variation curve in the sediment from Beppu Bay, Kyushu, Japan. *Rock Magnetism and Paleogeophysics*, *18*, 68–74.

Okada, M. (1995). Chapter 31. Detailed variation of geomagnetic field intensity during the late Pleistocene at Site 882. In D. K. Rea et al (Eds.), *Proceedings of the ocean drilling program, science results* (Vol. 145, pp. 469–474). College Station, TX: International Ocean Discovery Program.

Pan, Y., Zhu, R., Shaw, J., Liu, Q., & Guo, B. (2001). Can relative paleointensity be determined from the normalized magnetization of the wind-blown loess of China? *Journal of Geophysical Research*, *106*(B9), 19221–19232.

Panovska, S., & Constable, C. G. (2017). An activity index for geomagnetic paleosecular variation, excursions, and reversals. *Geochemistry, Geophysics, Geosystems*, *18*, 1366–1375. https://doi.org/10.1002/2016GC006668

Panovska, S., Finlay, C. C., Donadini, F., & Hirt, A. M. (2012). Spline analysis of Holocene sediment magnetic records: Uncertainty estimates for field modelling. *Journal of Geophysical Research*, *117*, B02101. https://doi.org/10.1029/2011JB008813

Panovska, S., Korte, M., Finlay, C. C., & Constable, C. G. (2015). Limitations in paleomagnetic data and modelling techniques and their impact on Holocene geomagnetic field models. *Geophysical Journal International*, *202*(1), 402–418.

Parker, R. L. (1994). *Geophysical inverse theory*. Princeton, NJ: Princeton University Press.

Parker, R. L., & Gee, J. S. (2002). Calibration of the pass-through magnetometer: II. Application. *Geophysical Journal International*, *150*(1), 140–152.

Pavón-Carrasco, F. J., Osete, M. L., Torta, J. M., & De Santis, A. (2014). A geomagnetic field model for the Holocene based on archaeomagnetic and lava flow data. *Earth and Planetary Science Letters*, *388*, 98–109.

Peck, J. A., King, J. W., Colman, S. M., & Kravchinsky, V. A. (1996). An 84-kyr paleomagnetic record from the sediments of Lake Bailkal, Siberia. *Journal of Geophysical Research*, *101*(B5), 11365–11385.

Peng, L., & King, J. W. (1992). A late Quaternary geomagnetic secular variation record from Lake Waiau, Hawaii, and the question of the Pacific nondipole low. *Journal of Geophysical Research*, *97*(B4), 4407–4424.

Reimer, P. J., Bard, E., Bayliss, A., Beck, J. W., Blackwell, P. G., Ramsey, C. B., et al. (2013). IntCal13 and Marine13 radiocarbon age calibration curves 0–50,000 years cal BP. *Radiocarbon*, *55*(04), 1869–1887.

Riethdorf, J.-R., Nürnberg, D., Max, L., Tiedemann, R., Gorbarenko, S. A., & Malakhov, M. I. (2013). Millennial-scale variability of marine productivity and terrigenous matter supply in the western Bering Sea over the past 180 kyr. *Climate of the Past*, *9*(3), 1345–1373.

Roberts, A. P. (2006). High-resolution magnetic analysis of sediment cores: Strengths, limitations and strategies for maximizing the value of long-core magnetic data. *Physics of the Earth and Planetary Interiors*, *156*(3–4), 162–178.

Roberts, A. P., Lehman, B., Weeks, R. J., Verosub, K. L., & Laj, C. (1997). Relative paleointensity of the geomagnetic field over the last 200,000 years from ODP Sites 883 and 884, North Pacific Ocean. *Earth and Planetary Science Letters*, *152*(1–4), 11–23.

Roberts, A. P., Tauxe, L., & Heslop, D. (2013). Magnetic paleointensity stratigraphy and high-resolution Quaternary geochronology: Successes and future challenges. *Quaternary Science Reviews*, *61*, 1–16.

Roberts, A. P., & Winklhofer, M. (2004). Why are geomagnetic excursion not always recorded in sediments? Constraints from post-depositional remanent magnetization lock-in modeling. *Earth and Planetary Science Letters*, *227*(3–4), 345–359.

Sato, T., Kikuchi, H., Nakashizuka, M., & Okada, M. (1998). Quaternary geomagnetic field intensity: Constant periodicity or variable period? *Geophysical Research Letters*, *25*(12), 2221–2224.

Sato, T., & Kobayashi, K. (1989). Long-period secular variations of the Earth's magnetic field revealed by Pacific deep-sea sediment cores. *Journal of Geomagnetism and Geoelectricity*, *41*(1), 147–159.

Schneider, D. A. (1993). An estimate of late Pleistocene geomagnetic intensity variation from Sulu Sea sediments. *Earth and Planetary Science Letters*, *120*(3–4), 301–310.

Schneider, D. A., & Mello, G. A. (1996). A high-resolution marine sedimentary record of geomagnetic intensity during the Brunhes Chron. *Earth and Planetary Science Letters*, *144*(1–2), 297–314.

Schwartz, M., Lund, S. P., & Johnson, T. C. (1996). Environmental factors as complicating influences in the recovery of quantitative geomagnetic field paleointensity estimates from sediments. *Geophysical Research Letters*, *23*(19), 2693–2696.
Simon, Q., St-Onge, G., & Hillaire-Marcel, C. (2012). Late Quaternary chronostratigraphic framework of deep Baffin Bay glaciomarine sediments from high-resolution paleomagnetic data. *Geochemistry, Geophysics, Geosystems*, *13*, Q0AO03. https://doi.org/10.1029/2012GC004272
Singer, B. S. (2014). A quaternary geomagnetic instability time scale. *Quaternary Geochronology*, *21*, 29–52.
Singer, B. S., Guillou, H., Jicha, B. R., Laj, C., Kissel, C., Beard, B. L., et al. (2009). $^{40}Ar/^{39}Ar$, K-Ar and ^{230}Th-^{238}U dating of the Laschamp excursion: A radioisotopic tiepoint for ice core and climate chronologies. *Earth and Planetary Science Letters*, *286*(1–2), 80–88.
Singer, B. S., Jicha, B. R., He, H., & Zhu, R. (2014). Geomagnetic field excursion recorded 17 ka at Tianchi Volcano, China: New $^{40}Ar/^{39}Ar$ age and significance. *Geophysical Research Letters*, *41*, 2794–2802. https://doi.org/10.1002/2014GL059439
Snowball, I., Zillén, L., Ojala, A., Saarinen, T., & Sandgren, P. (2007). FENNOSTACK and FENNORPIS: Varve dated Holocene palaeomagnetic secular variation and relative palaeointensity stacks for Fennoscandia. *Earth and Planetary Science Letters*, *255*(1–2), 106–116.
Stockhausen, H. (1998). Geomagnetic paleosecular variation (0–13 000 yr BP) as recorded in sediments from the three maar lakes from the West Eifel (Germany). *Geophysical Journal International*, *135*(3), 898–910.
Stockhecke, M., Kwiecien, O., Vigliotti, L., Anselmetti, F. S., Beer, J., Çağatay, M. N., et al. (2014). Chronostratigraphy of the 600,000 year old continental record of Lake Van (Turkey). *Quaternary Science Reviews*, *104*, 8–17.
Stoner, J. S., Channell, J. E. T., & Hillaire-Marcel, C. (1995). Late Pleistocene relative geomagnetic paleointensity from the deep Labrador Sea: Regional and global correlations. *Earth and Planetary Science Letters*, *134*(3–4), 237–252.
Stoner, J. S., Channell, J. E. T., & Hillaire-Marcel, C. (1998). A 200 ka geomagnetic chronostratigraphy for the Labrador Sea: Indirect correlation of the sediment record to SPECMAP. *Earth and Planetary Science Letters*, *159*(3–4), 165–181.
Stoner, J. S., Channell, J. E. T., Hillaire-Marcel, C., & Kissel, C. (2000). Geomagnetic paleointensity and environmental record from Labrador Sea core MD95–2024: Global marine sediment and ice core chronostratigraphy for the last 110 kyr. *Earth and Planetary Science Letters*, *183*(1–2), 161–177.
Stoner, J. S., Channell, J. E. T., Hodell, D. A., & Charles, C. D. (2003). 580 kyr paleomagnetic record from the sub-Antarctic South Atlantic (Ocean Drilling Program Site 1089). *Journal of Geophysical Research*, *108*(B5), 2244. https://doi.org/10.1029/2001JB001390
Stoner, J. S., Laj, C., Channell, J. E. T., & Kissel, C. (2002). South Atlantic and North Atlantic geomagnetic paleointensity stacks (0–80 ka): Implications for inter-hemispheric correlation. *Quaternary Science Reviews*, *21*(10), 1141–1151.
Stott, L., Poulsen, C., Lund, S., & Thunell, R. (2002). Super ENSO and global climate oscillations at millennial time scales. *Science*, *297*(5579), 222–226.
Stuiver, M., & Grootes, P. M. (2000). GISP2 oxygen isotope ratios. *Quaternary Research*, *53*(03), 277–284.
Suganuma, Y., Okuno, J., Heslop, D., Roberts, A. P., Yamazaki, T., & Yokoyama, Y. (2011). Post-depositional remanent magnetization lock-in for marine sediments deduced from ^{10}Be and paleomagnetic records through the Matuyama-Brunhes boundary. *Earth and Planetary Science Letters*, *311*(1–2), 39–52.
Svensson, A., Andersen, K. K., Bigler, M., Clausen, H. B., Dahl-Jensen, D., Davies, S. M., et al. (2006). The Greenland Ice Core Chronology 2005, 15–42 ka. Part 2: Comparison to other records. *Quaternary Science Reviews*, *25*(23–24), 3258–3267.
Svensson, A., Andersen, K. K., Bigler, M., Clausen, H. B., Dahl-Jensen, D., Davies, S. M., et al. (2008). A 60 000 year Greenland stratigraphic ice core chronology. *Climate of the Past*, *4*(1), 47–57.
Tauxe, L. (2002). *Paleomagnetic principles and practice*. Dordrecht, The Netherlands: Kluwer Academic Publishers.
Tauxe, L., Steindorf, J. L., & Harris, A. (2006). Depositional remanent magnetization: Toward an improved theoretical and experimental foundation. *Earth and Planetary Science Letters*, *244*(3–4), 515–529.
Tauxe, L., & Wu, G. (1990). Normalized remanence in sediments of the western equatorial Pacific: Relative paleointensity of the geomagnetic field. *Journal of Geophysical Research*, *95*(B8), 12337–12350.
Tauxe, L., & Yamazaki, T. (2007). Paleointensities. In M. Kono (Ed.), *Treatise of geophysics, geomagnetism* (pp. 509–563). New York, NY: Elsevier.
Thouveny, N., Carcaillet, J., Moreno, E., Leduc, G., & Nérini, D. (2004). Geomagnetic moment variation and paleomagnetic excursions since 400 kyr BP: A stacked record from sedimentary sequences of the Portuguese margin. *Earth and Planetary Science Letters*, *219*(3–4), 377–396.
Thouveny, N., Creer, K. M., & Blunk, I. (1990). Extension of the Lac du Bouchet palaeomagnetic record over the last 120,000 years. *Earth and Planetary Science Letters*, *97*(1–2), 140–161.
Thouveny, N., de Beaulieu, J.-L., Bonifay, E., Creer, K. M., Guiot, J., Icole, M., et al. (1994). Climate variations in Europe over the past 140 kyr deduced from rock magnetism. *Nature*, *371*(6497), 503–506.
Thouveny, N., & Williamson, D. (1988). Palaeomagnetic study of the Holocene and Upper Pleistocene sediments from Lake Barombi Mbo, Cameroun: First results. *Physics of the Earth and Planetary Interiors*, *52*(3–4), 193–206.
Tric, E., Valet, J. P., Tucholka, P., Paterne, M., Labeyrie, L., Guichard, F., et al. (1992). Paleointensity of the geomagnetic field during the last 80 000 years. *Journal of Geophysical Research*, *97*(B6), 9337–9351.
Turner, G. M., Howarth, J. D., de Gelder, G. I. N. O., & Fitzsimons, S. J. (2015). A new high-resolution record of Holocene geomagnetic secular variation from New Zealand. *Earth and Planetary Science Letters*, *430*, 296–307.
Valet, J. P., & Meynadier, L. (1993). Geomagnetic field intensity and reversals during the past four million years. *Nature*, *366*(6452), 234–238.
Valet, J.-P., Meynadier, L., & Guyodo, Y. (2005). Geomagnetic dipole strength and reversal rate over the past two million years. *Nature*, *435*(7043), 802–805.
Vigliotti, L. (2006). Secular variation record of the Earth's magnetic field in Italy during the Holocene: Constraints for the construction of a master curve. *Geophysical Journal International*, *165*(2), 414–429.
Vigliotti, L., Channell, J. E. T., & Stockhecke, M. (2014). Paleomagnetism of Lake Van sediments: Chronology and paleoenvironment since 350 ka. *Quaternary Science Reviews*, *104*, 18–29.
Vlag, P., Thouveny, N., Williamson, D., Rochette, P., & Ben-Atig, F. (2002). Paleomagnetic study of lacustrine sediments from Sun-Moon Lake, central Taiwan. *Western Pacific Earth Sciences*, *2*(1), 15–26.
Weeks, R. J., Laj, C., Endignoux, L., Mazaud, A., Labeyrie, L., Roberts, A. P., et al. (1995). Normalized natural remanent magnetization intensity during the last 240 000 years in piston cores from the central North Atlantic Ocean: Geomagnetic field intensity or environmental signal? *Physics of the Earth and Planetary Interiors*, *87*(3–4), 213–229.
Williams, T., Thouveny, N., & Creer, K. M. (1998). A normalized intensity record from Lac du Bouchet: Geomagnetic palaeointensity for the last 300 kyr. *Earth and Planetary Science Letters*, *156*(1–2), 33–46.

Xiao, W., Frederichs, T., Gersonde, R., Kuhn, G., Esper, O., & Zhang, X. (2016). Constraining the dating of late Quaternary marine sediment records from the Scotia Sea (Southern Ocean). *Quaternary Geochronology*, *31*, 97–118.

Xiaoqiang, Y., Heller, F., Nengyou, W., Jie, Y., & Zhihua, S. (2009). Geomagnetic paleointensity dating of South China Sea sediments for the last 130 kyr. *Earth and Planetary Science Letters*, *284*(1–2), 258–266.

Yamamoto, Y., Yamazaki, T., Kanamatsu, T., Ioka, N., & Mishima, T. (2007). Relative paleointensity stack during the last 250 kyr in the northwest Pacific. *Journal of Geophysical Research*, *112*, B01104. https://doi.org/10.1029/2006JB004477

Yamazaki, T. (1984). Thickness of the lock-in zone of post-depositional remanent magnetization in deep-sea silicious clay. *Rock Magnetism and Paleogeophysics*, *11*, 85–90.

Yamazaki, T. (1999). Relative paleointensity of the geomagnetic field during Brunhes Chron recorded in North Pacific deep-sea sediment cores: Orbital influence. *Earth and Planetary Science Letters*, *169*(1–2), 23–35.

Yamazaki, T., Abdeldayem, A. L., & Ikehara, K. (2003). Rock-magnetic changes with reduction diagenesis in Japan Sea sediments and preservation of geomagnetic secular variation in inclination during the last 30,000 years. *Earth, Planets and Space*, *55*(6), 327–340.

Yamazaki, T., & Ioka, N. (1994). Long-term secular variation of the geomagnetic field during the last 200 kyr recorded in sediment cores from the western equatorial Pacific. *Earth and Planetary Science Letters*, *128*(3–4), 527–544.

Yamazaki, T., Ioka, N., & Eguchi, N. (1995). Relative paleointensity of the geomagnetic field during the Brunhes Chron. *Earth and Planetary Science Letters*, *136*(3–4), 525–540.

Yamazaki, T., Kanamatsu, T., Mizuno, S., Hokanishi, N., & Gaffar, E. Z. (2008). Geomagnetic field variations during the last 400 kyr in the western equatorial Pacific: Paleointensity-inclination correlation revisited. *Geophysical Research Letters*, *35*, L20307. https://doi.org/10.1029/2008GL035373

Yamazaki, T., & Oda, H. (2005). A geomagnetic paleointensity stack between 0.8 and 3.0 Ma from equatorial Pacific sediment cores. *Geochemistry, Geophysics, Geosystems*, *6*, Q11H20. https://doi.org/10.1029/2005GC001001

Yang, X., Liu, Q., Duan, Z., Su, Z., Wei, G., Jia, G., et al. (2012). A Holocene palaeomagnetic secular variation record from Huguangyan maar Lake, southern China. *Geophysical Journal International*, *190*(1), 188–200.

Zheng, Y., Zheng, H., Deng, C., & Liu, Q. (2014). Holocene paleomagnetic secular variation from East China Sea and a PSV stack of East Asia. *Physics of the Earth and Planetary Interiors*, *236*, 69–78.

Zhu, R., Gu, Z., Huang, B., Jin, Z., Wei, X., & Li, C. (1994). Geomagnetic secular variations and climate changes since 15,000 a B.P., Beijing region. *Science in China Series B*, *37*(8), 984–990.

Ziegler, L. B., & Constable, C. G. (2015). Testing the geocentric axial dipole hypothesis using regional paleomagnetic intensity records from 0–300 ka. *Earth and Planetary Science Letters*, *423*, 48–56.

Ziegler, L. B., Constable, C. G., Johnson, C. L., & Tauxe, L. (2011). PADM2M: A penalized maximum likelihood model of the 0–2 Ma palaeomagnetic axial dipole moment. *Geophysical Journal International*, *184*(3), 1069–1089.